2011

Using water balance models to approximate the effects of climate change on spring catchment discharge : Mt. Hanang, Tanzania

Randall E. Fish
Michigan Technological University

Recommended Citation

USING WATER BALANCE MODELS TO APPROXIMATE THE EFFECTS OF CLIMATE CHANGE ON SPRING CATCHMENT DISCHARGE: MT. HANANG, TANZANIA

Randall E. Fish

A THESIS

Submitted in partial fulfillment of the requirements for the degree of

MASTER OF SCIENCE

Geology

MICHIGAN TECHNOLOGICAL UNIVERSITY

2011

This thesis, "Using Water Balance Models to Approximate the Effects of Climate Change on Spring Catchment Discharge: Mt. Hanang, Tanzania," is hereby approved in partial fulfillment of the requirements for the Degree of MASTER OF SCIENCE IN GEOLOGY.

Department of Geological and Mining Engineering and Sciences

Signatures:

Thesis Advisor   _____

Dr. John Gierke

Department Chair   _____

Dr. Wayne Pennington

Date   _____

TABLE OF CONTENTS

LIST OF FIGURES

LIST OF TABLES

ACKNOWLEDGEMENTS

ABSTRACT

This project addresses the potential impacts of changing climate on dry-season water storage and discharge from a small, mountain catchment in Tanzania. Villagers and water managers around the catchment have experienced worsening water scarcity and attribute it to increasing population and demand, but very little has been done to understand the physical characteristics and hydrological behavior of the spring catchment. The physical nature of the aquifer was characterized and water balance models were calibrated to discharge observations so as to be able to explore relative changes in aquifer storage resulting from climate changes.

To characterize the shallow aquifer supplying water to the Jandu spring, water quality and geochemistry data were analyzed, discharge recession analysis was performed, and two water balance models were developed and tested. Jandu geochemistry suggests a shallow, meteorically-recharged aquifer system with short circulation times. Baseflow recession analysis showed that the catchment behavior could be represented by a linear storage model with an average recession constant of 0.151/month from 2004-2010. Two modified Thornthwaite-Mather Water Balance (TMWB) models were calibrated using historic rainfall and discharge data and shown to reproduce dry-season flows with Nash-Sutcliffe efficiencies between 0.86 and 0.91.

The modified TMWB models were then used to examine the impacts of nineteen, perturbed climate scenarios to test the potential impacts of regional climate change on catchment storage during the dry season. Forcing the models with realistic scenarios for average monthly temperature, annual precipitation, and seasonal rainfall distribution demonstrated that even small climate changes might adversely impact aquifer storage conditions at the onset of the dry season. The scale of the change was dependent on the direction (increasing vs. decreasing) and magnitude of climate change (temperature and precipitation).

This study demonstrates that small, mountain aquifer characterization is possible using simple water quality parameters, recession analysis can be integrated into modeling aquifer storage parameters, and water balance models can accurately reproduce dry-season discharges and might be useful tools to assess climate change impacts. However, uncertainty in current climate projections and lack of data for testing the predictive capabilities of the model beyond the present data set, make the forecasts of changes in discharge also uncertain. The hydrologic tools used herein offer promise for future research in understanding small, shallow, mountainous aquifers and could potentially be developed and used by water resource professionals to assess climatic influences on local hydrologic systems.

1   INTRODUCTION

The Intergovernmental Panel on Climate Change (IPCC) states that the availability and distribution of freshwater resources will be greatly affected by climate change and the vulnerability to water scarcity that populations currently experience could increase (Parry 2007). Studies relating climate change and hydrology are becoming prevalent (see Leavesley 1994; Xu 1999), but few published studies focus on changes in African groundwater and the populations dependent upon it. The IPCC calls for expanded research on local impacts of climate change and finer-resolution assessments of changes in groundwater systems.

As a Peace Corps volunteer in Tanzania (2008-2010), I lived in a rural village that is dependent on discharge from a single spring for their domestic water supply. Personal interviews revealed villagers' perceptions were that dry-season water scarcity, experienced each year since around 2000, is worsening, and this is primarily caused by increased population and irrigation near the distribution point. An NGO is currently working to increase storage capacity and manage demand to alleviate the situation. This should ease water scarcity in the near future, but it does not account for the impacts climate change could have on water supply. According to the current climate data and analysis, East Africa will experience changes (the magnitude of which is uncertain) in regional climate (Parry 2007; Williams and Funk 2011).

Climate change continues, and with it our ability to predict changes is refined, but there is a need to develop simple tools that empower water resource managers to use the predictions to better understand and manage water sources. Complex models that generate outputs on continental scales are of little use for decision makers who are trying to allocate resources to alleviate local water scarcity. Rather, decision makers require readily applicable tools that can use climate predictions to accurately forecast local hydrologic changes.

Water balance models have been used to accurately simulate historical basin discharges (e.g., Xu and Singh 1998), forecast changes in discharges based on climate changes (e.g., Gleick 1987; Arnell 1992; Jiang et al. 2007), and are relatively straightforward to apply. Thus, water balance models could be an empowering tool for water resource managers to prepare for and mitigate the effects of regional climate change on their local hydrologic resources.

This report offers insight into how such a tool is created. The context for this development is a general physical characterization of a small catchment on Mt. Hanang, Tanzania and a method of incorporating discharge data into water balance models to improve model accuracy. Two water balance models are developed, calibrated, and then

forced with perturbed climate scenarios to assess relative future changes in dry-season catchment storage.

1.1 Literature Review

This review briefly describes springs and groundwater research in Tanzania, water balance models, recession analysis, and East-African climate patterns.

1.1.1 Groundwater & Springs

Precipitation infiltrating the earth as groundwater can encounter many heterogeneous layers of rock and soil. Porous and permeable layers that can store and transmit large volumes of groundwater are called aquifers. Springs occur where groundwater moving through an aquifer intersects the land surface due to changes in geology and/or topography, and groundwater emerges from a discrete source or 'seeps' (Bryan 1919) as shown in Figure 1.1.

Springs are characterized by many criteria, but the steep, mountainous site for this study is thought to be dominated by three types: fracture, contact, and depression springs. Fracture springs occur where fracture zones transmit water to the surface at some lower
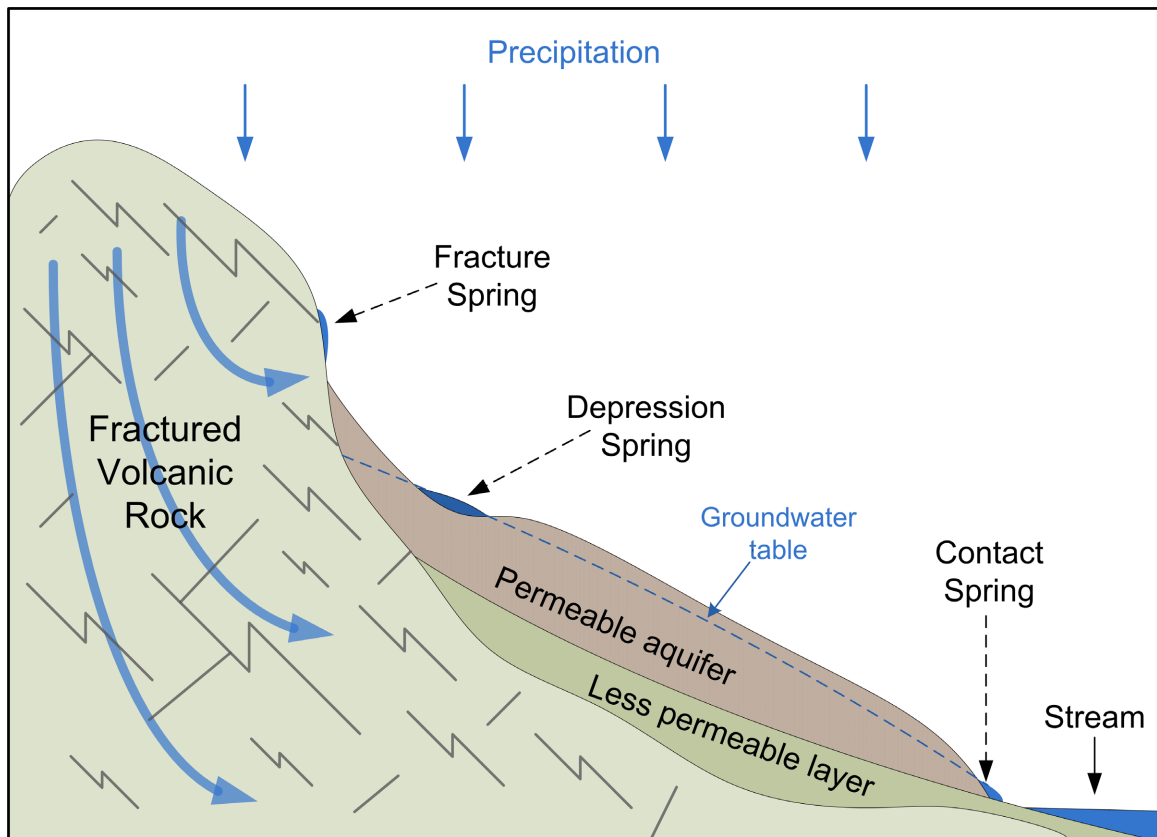
Figure 1.1 Conceptual diagram of springs

2

elevation. Fractures can hold large amounts of water and transmit it quickly, so fracture springs can have high discharges, but only produce water for a relatively short time. Contact springs are caused when an aquifer is underlain by an impermeable layer and groundwater is forced to move laterally until it intersects the land surface. Depression springs occur where the groundwater table meets the surface at a topographic low point and water is allowed to flow more easily along the surface (Fetter 2001). More information about spring characteristics and types is described in Bryan (1919).

Groundwater that emerges as a spring carries chemical and thermal signatures that provide insights about the aquifer(s) through which it passed, the altitude(s) at which it was recharged, and the depth(s) of and time spent in circulation (Manga 2001). Properties such as pH, electrical conductivity (EC), temperature, and isotopic abundance are routinely used to characterize the flow history and chemical evolution of spring water. Furthermore, the size and rate of spring discharge also indirectly describe local geology and aquifer recharge characteristics. Studying springs offers insights about both local and regional geologic activity, aquifer properties, and the processes and environment that the water experienced from recharge to discharge.

Groundwater research in Tanzania has primarily examined the characteristics of regional flow systems (Mul et al. 2007; Mckenzie et al. 2010) and the potential for groundwater resource development (JICA 2008). Analyzing the geochemistry and isotopes of water on Mt. Kilimanjaro, Mckenzie et al. (2010) found evidence for multiple flow systems with varying water qualities and ages. Mul et al. (2007), using chemical analysis and geological mapping, characterized the regional groundwater system in a mountain range and found evidence for two main components: a regional, tectonically controlled system, and a high-altitude, shallow system concentrated in debris-flow deposits. The Japan International Cooperation Agency (JICA) conducted an evaluation of the groundwater resources and potential for development in the Internal Drainage Basin, an area that spans from Arusha to Dodoma and covers 16% of Tanzania. JICA (2008) compiled meteorological, geological and hydrological data from various sources and concluded that areas along the Rift Valley and the adjacent volcanic mountains could be productive groundwater systems.

1.1.2   Water Balance Models
Water balances, which calculate catchment inputs and outputs, are another way of understanding the hydrologic setting and functioning of spring systems, as well as analyzing the sustainability of groundwater (Dingman 2002). This section outlines water balance approaches for characterizing near-surface hydrology and its applications to climate-change research.

3

The basic water balance equation (Dingman 2002) for a catchment without surface water inflows and no water abstractions nor diversions is:

$$P + G_{in} - (Q + ET + G_{out}) = \Delta S \qquad (1)$$

Where the variables represent input/output rates (volumetric fluxes) as volume of water per unit system area per unit time:

P = precipitation (L t^{-1})

G_{in} = groundwater inflow (L t^{-1})

Q = surface-water runoff (L t^{-1})

ET = evapotranspiration (L t^{-1})

G_{out} = groundwater outflow (L t^{-1})

ΔS = change in storage (L t^{-1})

Estimating the values for these parameters can be difficult, especially for incoming and outgoing fluxes of groundwater. The boundaries of the water budget are usually delineated to deliberately coincide with the watershed boundaries and surface-water and groundwater inflows are assumed to be zero. In addition, groundwater discharges are often thought to be small and are difficult to quantify, so they are commonly assumed to be negligible. The equation is then simplified as:

$$Q = P - ET - \Delta S \qquad (2)$$

When solved for consecutive periods of time, or time steps, it is deemed a water balance model.

Thornthwaite (1948) and Thornthwaite and Mather (1955) created some of the first water balance models, and since then many variations reflecting different applications, structures, and spatial and temporal scales have been developed (Leavesley 1994). The literature abounds with variations in modeling theory and techniques, and the reader is referred to Beven (2006) and Xu and Singh (1998) for more thorough reviews. In the Methods section of this report, the original Thornthwaite-Mather water balance model (TMWB) is reviewed. Here, the modified versions that were developed for climate impact studies (Alley 1984; Gleick 1987) and those actually applied to forecasting impacts of climate change on hydrological systems (Arnell 1992; Jiang et al. 2007) are reviewed.

Alley (1984) notes several issues with the TMWB model, including how it simulates overland flow, responds to temporal rainfall distribution, estimates water surpluses, and produces runoff in dry months. To account for runoff events during high-intensity storms, a parameter is added which immediately routes a portion of precipitation to runoff. If precipitation is disproportionally high at the end of the month, a modeler can adjust rainfall distributions so runoff is accurately generated in the present and next month. Alley (1984) incorporates a fraction, λ, which varies from catchment to catchment and represents the amount of monthly discharge carried over to the next month as surplus. This parameter is included because it ameliorates the TMWB model's inability to generate runoff unless soil moisture exceeds the field capacity. In Alley's simulations the TMWB model lacked the ability to simulate runoff in basins with consecutive months of soil moisture deficit, and while it reproduced annual flows well, monthly discharges were less accurate. Errors during the calibration period were found to be nearly equal to the errors during the prediction period.

Gleick (1987) modeled the Sacramento River Basin with a modified TMWB model that incorporates a storm runoff fraction and a watershed lag coefficient. The runoff fraction attempts to reproduce runoff that never enters soil moisture storage. Its value is a specified percentage of total precipitation: 10% in the first months of the rainy season as soil moisture is initially recharging. After two months, soil moisture is assumed to have significantly recharged, then the fraction increases to 30%. The basin is very large (41,000 km^2), so the watershed lag function is added to account for delays between rainfall and runoff. Gleick (1987) uses a maximum soil moisture capacity value of 150 mm based on local estimates. The model reproduced monthly flows to within 3-4% of observed values from a 50-year data set.

Arnell (1992) incorporates a runoff fraction for initial precipitation and λ in a modified TMWB model to study 15 large, humid temperate catchments. Seven arbitrarily selected scenarios were tested in which precipitation totals were incrementally increased and the seasonal distributions altered. A strong correlation was observed between the overall impact of changing precipitation on discharge and the seasonal distribution of that precipitation. For example, when more precipitation occurs in winter when evapotranspiration is low, more recharge enters soil moisture storage than if that precipitation increase occurs during high ET periods. When precipitation increased 10%, total discharge increased from 13-30%, and increases were higher still when precipitation increases were concentrated in the winter. Arnell (1992) stresses two shortcomings of the methodology: 1) the inherent assumption that models calibrated to historic data will remain accurate under future climate conditions, and 2) a limitation of using historic precipitation records is that previous extreme events maintain their strong influence in the future scenarios.

Jiang et al. (2007) used the TMWB model to reproduce historical discharges from a large basin with 90% accuracy. The model was forced with arbitrary climate scenarios (changes in precipitation and temperature), and the results were compared to outputs from five other hydrologic models. The TMWB model and two others produced similar results that were always the most extreme of the models. If temperature increased 1 °C and precipitation decreased 10% and 20%, mean annual flow decreased 20% and 40%, respectively. An increase of 4 °C concomitant with precipitation decreases of 10% and 20% lead to decreases in mean annual discharges of 32% and 50%, respectively. Even with no changes in precipitation, discharges decreased 15% for a 4 °C increase. Changes in runoff were found to be more sensitive to changes in precipitation than temperature. Jiang et al. (2007) concluded that different models will produce different results when forced with perturbed climate scenarios, and warn that results from a single model cannot be thought of as absolutely accurate representations.

The TMWB was chosen for this research because it provides accurate estimations of surface runoff using only precipitation and temperature data. It is a simple model with only two, easily calibrated parameters, and it has already been established as a tool for estimating the hydrological effects of climate change.

1.1.3 Recession Analysis

Analyzing a spring hydrograph, a plot of discharge versus time, is often done to determine aquifer properties and behavior. Specifically, the rate of decrease, or recession, in discharge after a peak represents a summation of multiple catchment runoff and storage components: overland flow, interflow and baseflow (Smakhtin 2001) (see Figure 1.2). After a given period of time (typically hours or days), depending on the catchment area and drainage network, it is assumed that the faster flow components of overland and interflow have completely drained and only baseflow from aquifer storage remains. Once incidences of baseflow are confidently isolated in a hydrograph, recession analysis examines the rate of discharge reduction to make inferences about the physical characteristics of the aquifer and its storage properties.

Boussinesq (1904) is credited with the first mathematical solutions to the baseflow recession problem. In their extensive reviews of baseflow recession analysis, Hall (1968) and Tallaksen (1995) examine the various forms that Boussinesq equations may take. The linear solution, which is based on Dupuit's assumptions[1] and assumes no capillary

---

[1] The Dupuit (1863) assumption simplified the analysis of aquifer drainage by assuming that groundwater only moves horizontally in an aquifer.
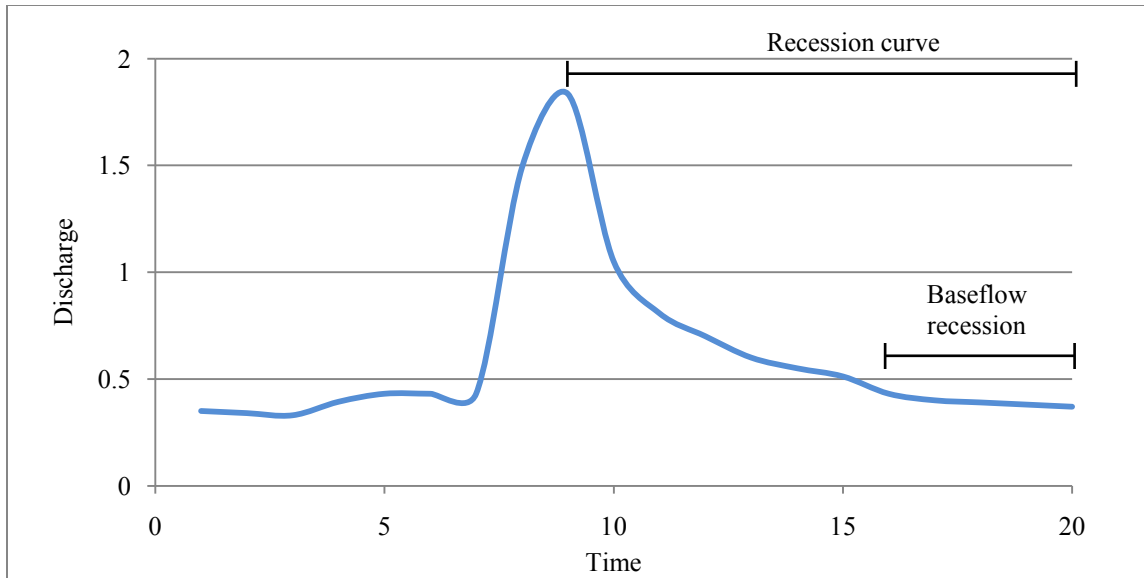
Figure 1.2 Spring hydrograph example

action, is the most common and simplest formulation to use for recession analysis, so it is the only solution described here (Hall 1968):

$$Q_t = Q_0 e^{-kt} \qquad (3)$$

where

Q_t = discharge at time t (m^3 t^{-1})

Q_0 = initial (t=0) discharge (m^3 t^{-1})

k = recession constant (t^{-1})

Boussinesq's equations are for unconfined aquifers under ideal conditions, which assume no recharge, evapotranspiration, nor leakage. This solution will only be valid for a system where the log-transformed discharge plots as a straight line against time (Hall 1968). The recession constant relates to a linear storage-outflow function as follows (Tallaksen 1995):

$$Q = kS \qquad (4)$$

where

S = catchment storage (m^3)

Using these equations to define aquifer characteristics implies that there is only one storage reservoir contributing to flow, but this is probably rarely the case (Tallaksen

1995). While some research has shown that some reservoirs behave nonlinearly (Wittenberg 1999), Brandes et al. (2005) noted that on time scales longer than one week, reservoirs often behave linearly and are thus accurately represented with Eqs. (3) and (4).

Many authors have used recession analysis to achieve a variety of aims. Bako and Owoade (1988) were able to accurately forecast low flows for temperate catchments. Moore (1992) used recession analysis to estimate aquifer properties such as transmissivity (hydraulic conductivity multiplied by aquifer thickness) and specific yield. Wittenberg and Sivapalan (1999) were able to estimate all the parameters for a catchment water balance, and Lamb and Beven (1997) showed that recession analysis could be used to conceptualize catchment storage parameters and to calibrate hydrological models.

The applicability of recession constants to catchments of varying geologic structure has also been explored. Zecharias and Brutsaert (1988) found that recession constants in the Appalachian Mountains were well correlated to catchment geomorphic features. Mendoza et al. (2003) successfully calculated transmissivity in a mountainous, fractured, semi-arid basin with a version of Eq. (3). Brandes et al. (2005) performed recession analysis for 24 small, morphologically diverse basins in Pennsylvania and found that recession constants were strongly correlated to drainage density and soil groups. In general, the steeper the slope and the greater the drainage density of a catchment, the higher the recession constant will be (Zecharias and Brutsaert 1988; Brandes et al. 2005).

1.1.4   East Africa Climate: Past and Future

Analysis of historic trends in East African precipitation patterns demonstrate a largely stable system that has experienced moderately increased precipitation from the 1970s through 2000 (Hulme et al. 2001; Nicholson 2001). Recent research correlates changes in regional precipitation to changes in Pacific and Indian Ocean sea-surface temperatures (SST) such as El Niño-Southern Oscillation (ENSO) and Indian Ocean Dipole (IOD) anomalies (Paeth and Hense 2006; Abram et al. 2007). ENSO and positive IOD events tend to increase precipitation in the early parts of the rainy season (October to January) (Schreck and Semazzi 2004; Ummenhofer et al. 2010) but show weaker influences later in the dry season (Ropelewski and Halpert 1996).

The IPCC consolidated the limited research available about East African climate change and postulates a 7% net increase in precipitation occurring during December to February and a regional temperature increase of 3.7 °C by 2080 for moderate emissions scenarios. The panel notes the difficulty in simulating the contributing variables, and states that precipitation predictions are far more uncertain than temperature (Parry 2007).

After the IPCC report was published, Conway et al. (2007) compared six general circulation models (GCM), based on temperature increases of 3.3 °C, that were coupled

to simulations of Indian Ocean SST anomalies. The results exemplify the continued uncertainty of global climate predictions: two models showed increased precipitation, two decreased, and two produced stable regimes. All of the increases and decreases were within 5-10% of historical mean annual rainfall. Williams and Funk (2011) found that when a change in regional Walker circulation patterns related to warming Indian Ocean SST is incorporated in GCMs, precipitation increases over the oceans but decreases over East Africa from March to June. The simulations suggest that East African climate will become drier as temperature increases but do not offer a single, quantified prediction.

1.2   Objectives

Livelihoods are greatly impacted by water scarcity, especially the health and well-being of women and children, and the following objectives are motivated by the need to address that water scarcity now and in the future. This research aims to help ameliorate local water scarcity by characterizing the aquifer and modeling the catchment.

Objective 1: Conceptually characterize the aquifer system using basic water quality parameters and recession analysis.

A basic understanding of the functionality of an aquifer, the origin of its water, and its recharge characteristics is necessary for water resource managers to appropriately protect and manage the supply. This information can then be used to supplement traditional techniques to conceptualize and parameterize physically-based models of the catchment.

Objective 2: Create a water balance model that is conceptually sound and accurately reproduces the mean dry-season discharge of the project catchment.

Parametrically simple water balance models are not often utilized in small catchments or parameterized with supplementary physical data. The primary goal for this work is to demonstrate that such models can be applied at small scales and that parameterization is assisted by using geochemical data and recession analysis.

Objective 3: Use the water balance model to assess the relative effects of changes in temperature and precipitation on aquifer storage, offering some insight about how future climate conditions may impact spring flows.

The ability to forecast changes in future groundwater supply from changes in climate has the potential to help water resource planners better allocate water resource development funds. Water balance models are tools that, as climate predictions become more refined, could easily be used by managers in developing nations to regularly reevaluate community water supplies. If a catchment is predicted to be significantly impacted by changing climate, development and assistance funds could be used to develop new sources or channeled to those affected before water scarcity occurs.

2   PROJECT SITE (S 4°25' E 35°20')

2.1   Geography & Geology

Mt. Hanang (elevation 3,418 m) is located at the southernmost tip of the eastern branch of the Great Rift Valley in Hanang District, Manyara region, Tanzania (see Figure 2.1) (Greenway 1955). The semi-arid climate is characterized by a highly variable rainy season from November through May, with an average rainfall of 600-900 mm and an average evapotranspiration of 2000 mm (JICA 2008). Precipitation originates from Northeasterly winds and the Eastern slopes have considerably more vegetation and water availability than the Western side. The Mt. Hanang Forest Reserve was established in 1984 to protect mountain water sources from human encroachment, and this theoretically limits cultivation and logging to elevations below 2000 m (see Figure 2.2).

Figure 2.1   Map of Tanzania (Courtesy of the University of Texas Libraries, The University of Texas at Austin, see Appendix 8.1 for usage information)

10
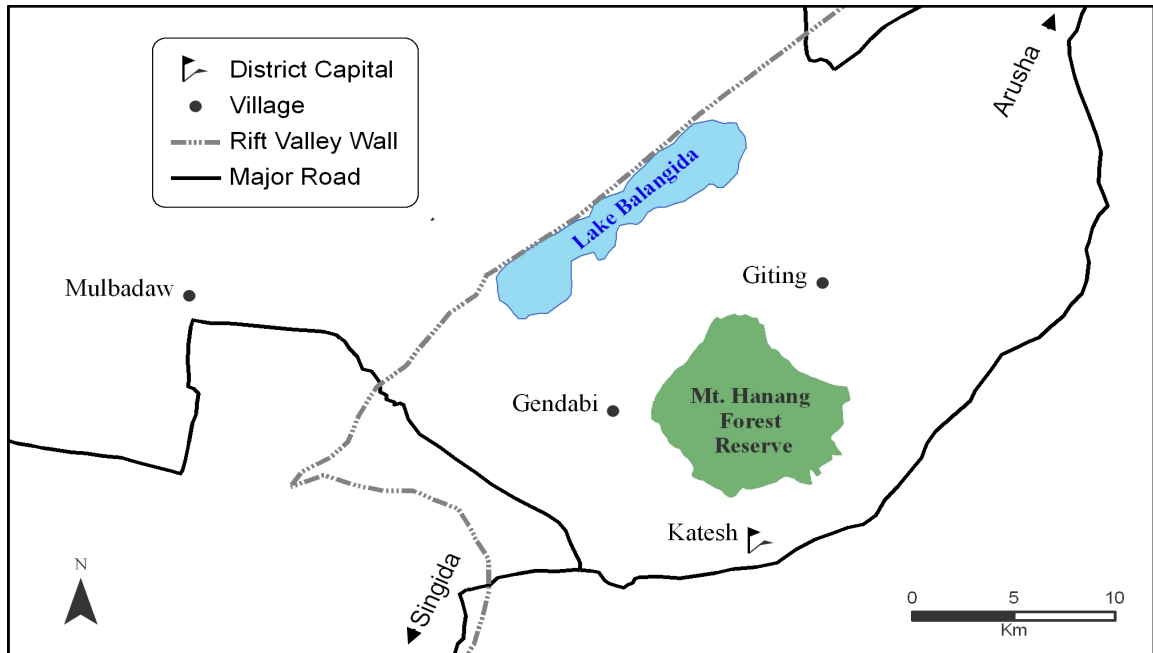
Figure 2.2 Map of the Hanang district

Mt. Hanang is an extinct stratovolcano, thought to have last erupted during the Pleistocene (Dawson 2008). The core of Hanang is composed of nephelinitic tuffs and agglomerates, whereas the slopes are characterized by nephelinitic lavas and carbonatitic tuffs (Dawson 2008) (see Figure 2.3). The body of the mountain is defined by a large, south-sloping valley, hypothesized to be the remnants of a crater collapse (Thomas 1966). The surrounding red clay and sandy soils are mostly weathered material from these formations (Thomas 1966). Steep ravines carve Hanang's circumference, and Figure 2.2 is a photograph from a ravine that shows lithographic units that exhibit variable thicknesses and fracturing.

2.2 People

Census data from 2002 estimates the Hanang District population is 225,000 and growing annually at a rate of 4%. The villages surrounding the mountain are inhabited by two tribal groups: the agricultural Iraqq and pastoralist Barabaig. Historically the area was dominated by cattle-raising, semi-nomadic Barabaig, but as fertile lands to the north became overpopulated, the Iraqq migrated to Hanang and began cultivating its fertile soils. Both tribes now practice a balanced agro-pastoralism that is animal-powered and focuses on maize and bean production. Some Barabaig have been reluctant, though, to adopt this sedentary life, and still migrate seasonally in search of scarce water and pasture.

11
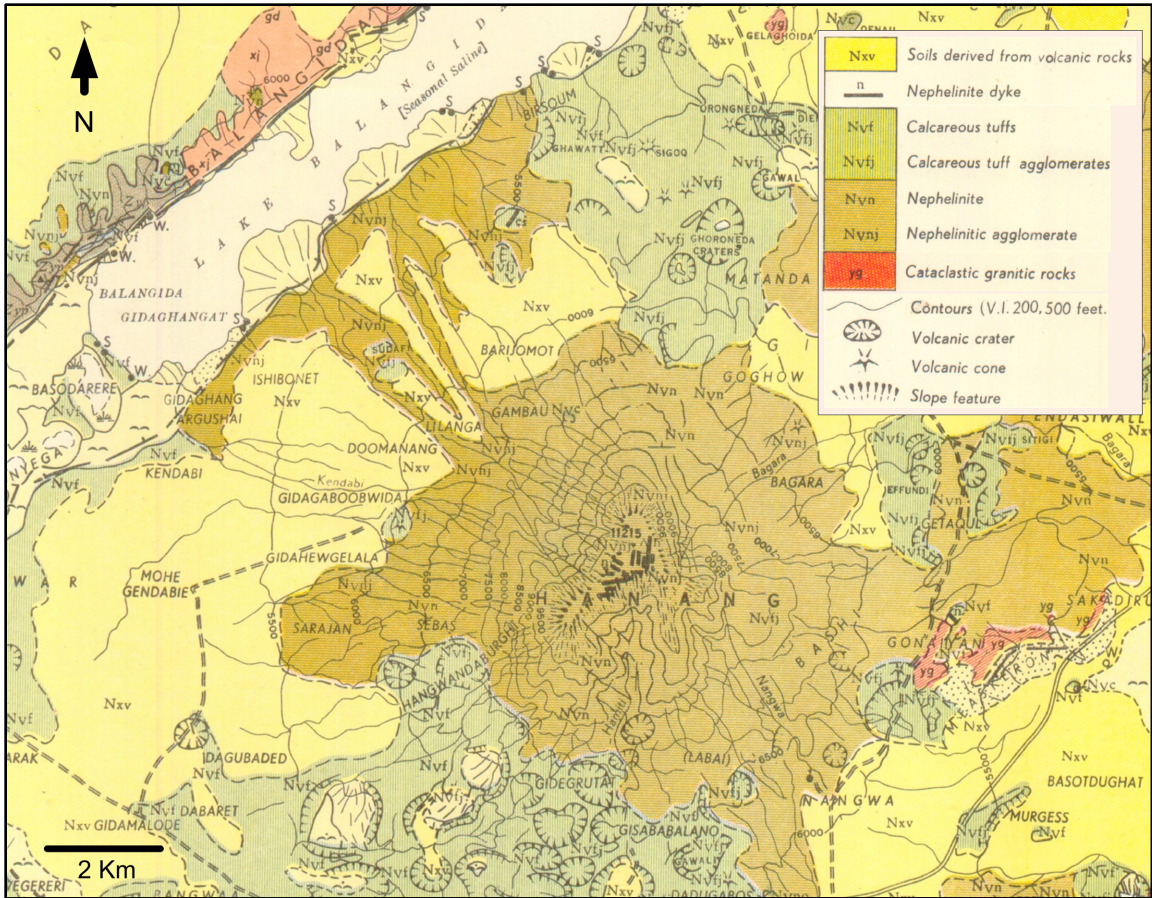
Figure 2.3 Hanang geologic map (Courtesy of the Geological Survey of Tanzania, see Appendix 8.2 for usage information)

2.3 Hydrology

Hanang District lies in the Bahi Sub-Basin in Tanzania's Internal Drainage Basin (IDB). In their assessment of groundwater resources in the IDB, JICA (2008) estimated the sub-basin area as 26,500 km^2. The Northern boundary of Bahi Sub-Basin is defined by the rift valley wall, which, after being uplifted some 500 m, created depressions where seasonal salt lakes develop. Infiltration rates are near zero for the IDB due to low annual precipitation and high potential evapotranspiration. Rainy season runoff in the sub-basin averages only 2-11% of precipitation (JICA 2008). Mt. Hanang is only briefly mentioned in the JICA report, and although deemed an unimportant site for development of groundwater resources (i.e., wells), its many springs and streams are the only source of domestic freshwater for almost half the residents of Hanang District.

The Tanzania Ministry of Water conducted an inventory of local water supplies (titled *Arusha Region Water Master Plan* or AWMP 2000) and concluded that within the forest area of Mt. Hanang there are ten significant springs and spring-dominated streams, and

many others below the forest boundary (see Figure 2.4). Personal observations suggest that most of the springs are contact and depression springs caused by loose deposits on Hanang's steep slopes, the heavily-fractured volcanic core, and the heterogeneous permeability of its stratigraphic profile. Two main drainage components were identified: low-discharge, gravitational seepage from saturated slopes and high-discharge transmission through fractured volcanic rocks.
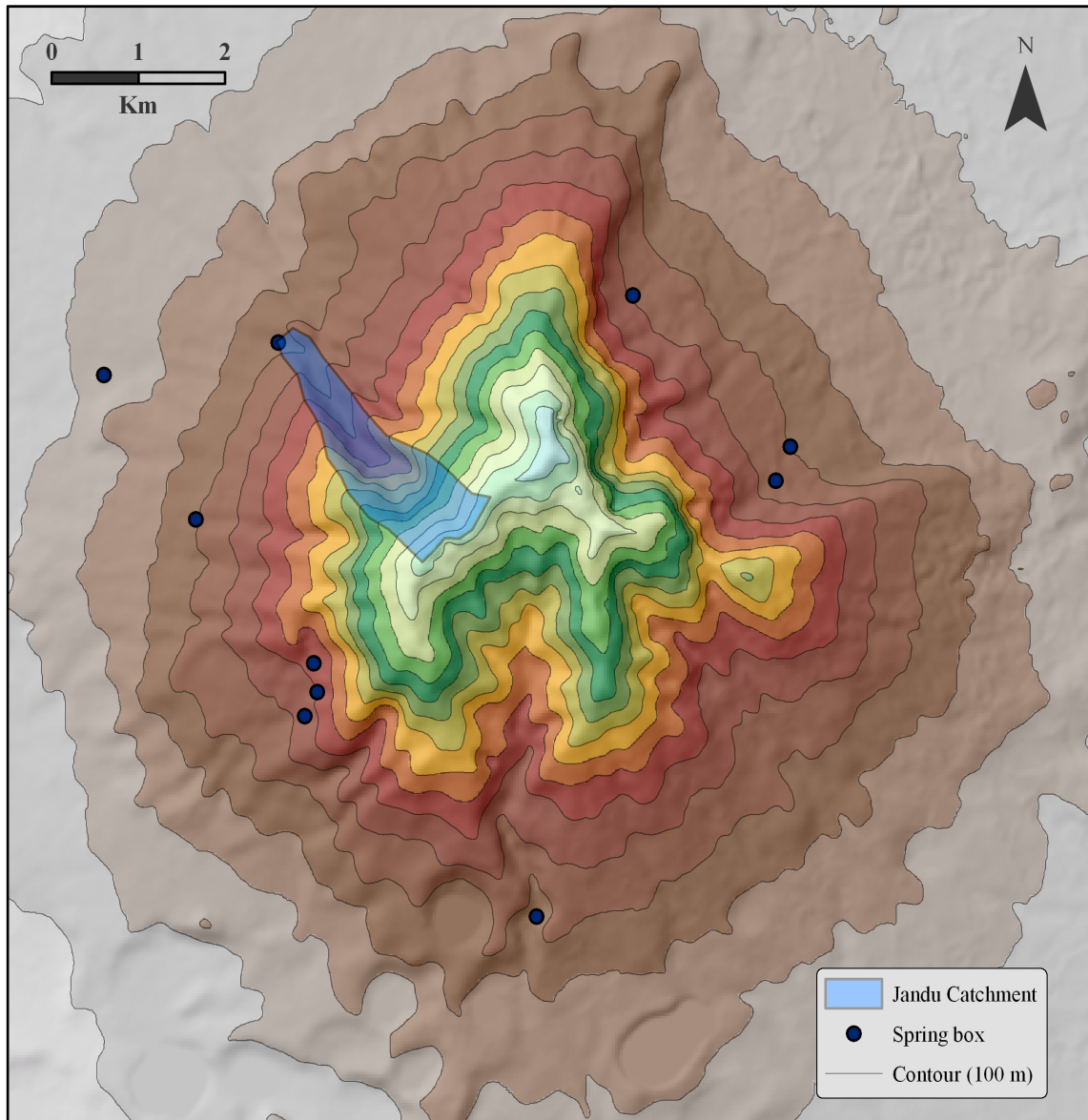
Figure 2.4 Mt. Hanang contour map, spring locations, and Jandu catchment outline (Courtesy of the U.S. Geological Survey, 2011, see Appendix 8.3 for usage information)

Most springs were sampled by the author and found to be fresh with pH ranges from 7.1 to 8.5 and electrical conductivities between 116 and 396 µS. All springs and streams are captured with concrete spring boxes and gravity-fed to surrounding villages, supplying a total of about 100,000 people with domestic freshwater (AWMP 2000). Himet stream, which drains the central crater, is the most productive with an average discharge of 2000 m^3d^{-1} and supplies water to 22,000 residents in Katesh Town. AWMP (2000) notes that Jandu stream, the second most productive stream on the mountain, is the only one with long-term, continuous discharge records.

2.4   Jandu Stream

Jandu stream flows year round from a small catchment on the Northwest slope of Mt. Hanang (see Figure 2.5). Assuming that spring recharge zone boundaries coincide with topographic boundaries, ArcGIS9.2 was used to calculate the catchment area and gave a value of 2.03 km^2 using an ASTER digital elevation model (30 m resolution).

The ravine in which Jandu flows is steep, and the thick vegetation repels efforts to enter the watershed area, especially during the wet season. Vegetation in the catchment valley is composed of sparse, large hardwoods and dense thickets, and upslope it transitions to Acacia scrubland. The entire watershed is within the Hanang Forest Reserve, and although instances of illegal logging were observed, the catchment shows minimal impacts from human development.

Field investigations of the lower-catchment area revealed numerous small streams coalescing from seeps all along the ravine. It is hypothesized that further up the catchment, there are areas of fractured rock that contribute larger water volumes to these streams near their headwaters. This hypothesis stems from two pieces of evidence: 1) Some water at other Hanang streams, which the author was able to observe near the source, emerges from large fissures and fractures, often at the base of a large rock face, and 2) Jandu catchment has multiple waterfalls at higher elevations, along open rock faces, that were observed draining water during the wet season and then ceasing in the dry season.

In 1989, a Canadian organization developed a concrete reservoir and gravity distribution system that transports water from Jandu stream to seven farms above the rift valley wall. Pictured in Figure 2.6, the reservoir (S 4° 25' 23", E 35° 22' 25", 2050 mamsl) incorporates a v-notch weir, a slotted-intake pipe, and a 150 m^3 storage tank. AWMP (2000) states that the system capacity is 847 m^3d^{-1} and serves an estimated population of 4,000. The system captures most catchment runoff, but the intake pipe clogs with organic debris, so a full-time maintenance manager cleans the intake and records daily weir levels. These records are the basis for the analysis in this report.

Figure 2.5 Jandu catchment area seen from caretaker's home

Figure 2.6 Jandu reservoir and weir. This photo was taken during the wet season.

3   METHODS

3.1   Field Data Collection

Collected field data includes basic water quality parameters, water samples for isotope and geochemical analysis, historic discharge and precipitation measurements, and personal interviews. Basic water quality parameters of pH, electrical conductivity (EC), and temperature were measured monthly from February to September 2010 with a Hanna Instruments™ 98129 Combo Meter (Woonsocket, RI). Precisions are within pH ±0.05, temperature ±0.5°C, and EC ±2% F.S.

Spring water samples collected in May and September 2010 were analyzed in November 2010 by the Michigan Department of Community Health (Houghton, MI) for alkalinity and hardness and some anions and cations (Cl^-, F^-, Na^+, $SO_4{}^{2-}$). In March, May, and September 2010, spring samples were collected following Kendall and McDonnell (1998) for isotope analysis. In December 2010 the samples were analyzed for ^2H and ^{18}O isotope compositions by the Department of Earth and Space Sciences at the University of Washington (Seattle, WA) using a Picarro L1102-i Cavity Ringdown Laser (Sunnyvale, CA). Isotope data and discussion is found in Appendix 8.4 and is not mentioned further in the report.

Figure 3.1 Field data tools

Jandu stage-height measurements at the v-notch weir were recorded each morning by the maintenance manager, and records from 2004-2010 were copied from his notebook. Stage-height measurements (cm) are converted to flow (discharge) in liters per second (Lps) using the stage-discharge equation given by AWMP (2000):

$$Q = 1.382h^{2.5} \tag{5}$$

where:

Q = discharge (m^3 s^{-1})

h = stage height (cm)

Katesh precipitation data is from the Department of Agriculture in Katesh (S 4°31'5", E 35°22'36") where the station elevation is 1721 m. Daily records were available from 2007 to 2010 and monthly records from 1985-2010. The 2003 records were absent. The same data was found in AWMP (2000) but with some discrepancies, so the Department of Agriculture records are used in this research

Semi-structured, personal interviews were conducted in June 2010 under Michigan Technological University IRB Approval M0570. Questions concerned water consumption, the current state of water infrastructure, a current project to improve the water distribution system, and opinions on paying for water. The data is not discussed further, but helped the author to better understand local water scarcity and its causes.

3.2   Recession Analysis

The recession curve of a hydrograph represents a continuum of discharge components: surface runoff, interflow, and baseflow. By splitting the discharge record into two periods, one in which recharge occurs (wet season) and one with negligible recharge (dry season), the baseflow component is isolated, and decreases in discharge over time represent groundwater draining from aquifer storage.

Daily discharge measurements from 2004 to 2010 were aggregated to monthly discharges, and the logarithm of discharge plotted as a function of time in Microsoft Excel™. An exponential trend line was fit to the data, and the average recession constant (as given in Eq. 3) was derived from the trend line equation (see Figure 12). This is an average recession constant for all years, but was found to be identical when each dry season was computed individually and averaged.
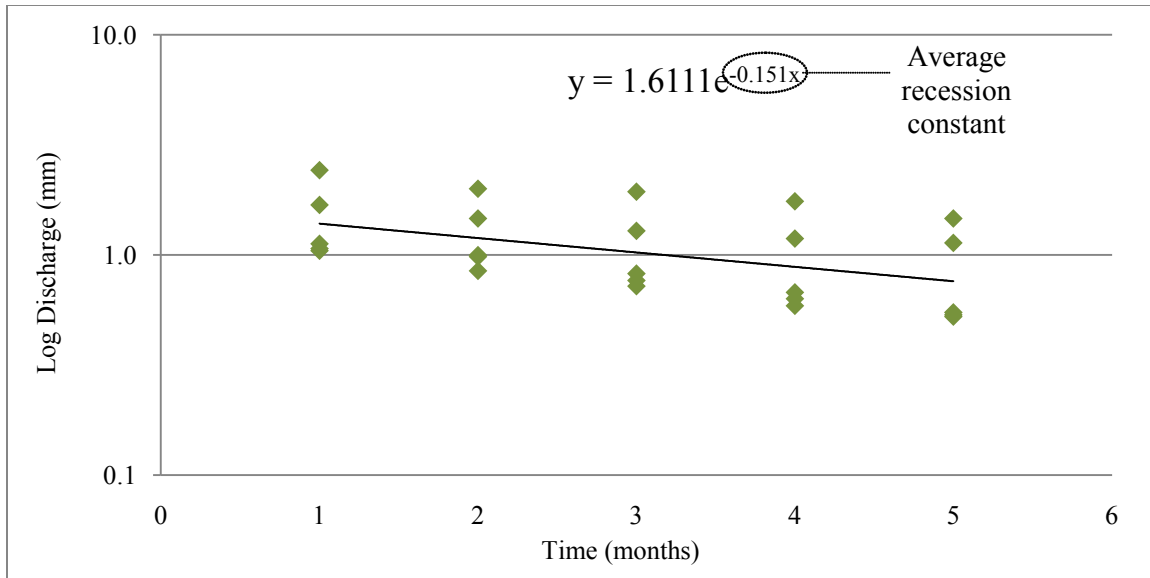
Figure 3.2 Graph of baseflow recession curve and fitted trend line

3.3 Thornthwaite-Mather Water Balance

The Thornthwaite-Mather Water Balance (TMWB) is a comprehensive water balance model for the rootzone of a homogenous catchment. This research applies a version of the TMWB, adapted from Dingman (2002), that uses the Hamon method to determine potential evapotranspiration. Appendix 8.5 outlines the governing equations. This section describes the primary logic conceptually.

The TMWB requires inputs of precipitation (P), temperature, latitude, and rootzone thickness and field capacity. The day length (based on latitude and month) and temperature are used to estimate monthly potential evapotranspiration (PET). Actual evapotranspiration (ET) will equal PET if sufficient water is available from P and soil moisture, otherwise the Hamon method is used to estimate ET from PET. When P exceeds PET, water enters soil moisture storage. Once the field capacity of the soil is exceeded, the excess becomes runoff/recharge (see Figure 3.3). The water remaining in soil moisture storage at the end of the month carries over to the next month.

The soil parameters are rootzone thickness and soil field capacity, which are present in the model only as a product and can thus be calibrated as a single entity. Rootzone thickness reflects the average depth of vegetation roots, and corresponds to the effective depth from which ET occurs. Soil field capacity, related to porosity and soil-water tension, is defined as "the water content below which further decrease occurs at a 'negligible' rate" (p235, Dingman, 2002). These parameters are multiplied and lumped together to estimate a maximum soil moisture storage capacity, henceforth referred to as *TMWB soil$_{max}$*. This becomes the total soil moisture storage volume of the system.

18
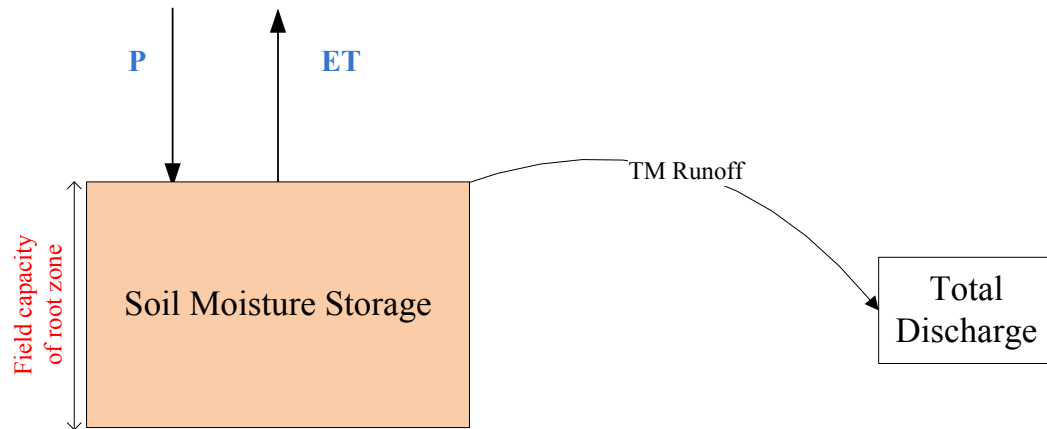
Figure 3.3 Thornthwaite-Mather model (TMWB) conceptualization. Note that runoff is only produced when soil moisture storage exceeds capacity.

While the TMWB provides estimates of evapotranspiration, the inputs and outputs of each month must balance. The runoff of excess precipitation is treated as immediate and does not allow the precipitation in a given month to contribute to discharge in subsequent months, essentially ignoring any discharge from aquifer storage. Hence, there is no mechanism to generate runoff in months without precipitation. The Jandu catchment has stream flow during the dry season, so two alternative models were developed to address the lack of storage.

3.3.1 Model 1

An aquifer storage component was first added to the TMWB model to simulate catchment interflow and baseflow. All of the TMWB-estimated runoff is routed to aquifer storage, which drains according to a single baseflow-recession-constant parameter (α). There is no maximum capacity for aquifer storage and it is not affected by evapotranspiration. This function allows temporally variable drainage of soil moisture, but wet-season flows are not well represented and the initial volume of water in storage is exaggerated.

Improved simulation of wet-season flows and water storage was obtained by incorporating a wet-season, rainfall-runoff component that more effectively generates rapid runoff, which is observed during rains (see Figure 3.4). The 'runoff constant' function (*RC*) is calculated for each year as a percentage of total annual precipitation, and all TMWB runoff is routed through this function before entering aquifer storage. This is an appropriate model addition because the annual wet-season precipitation and mean wet-season discharge at Jandu are minimally correlated (r^2=0.54). The *RC* is only active in the wet season and stipulates that TMWB runoff, less than or equal to the computed
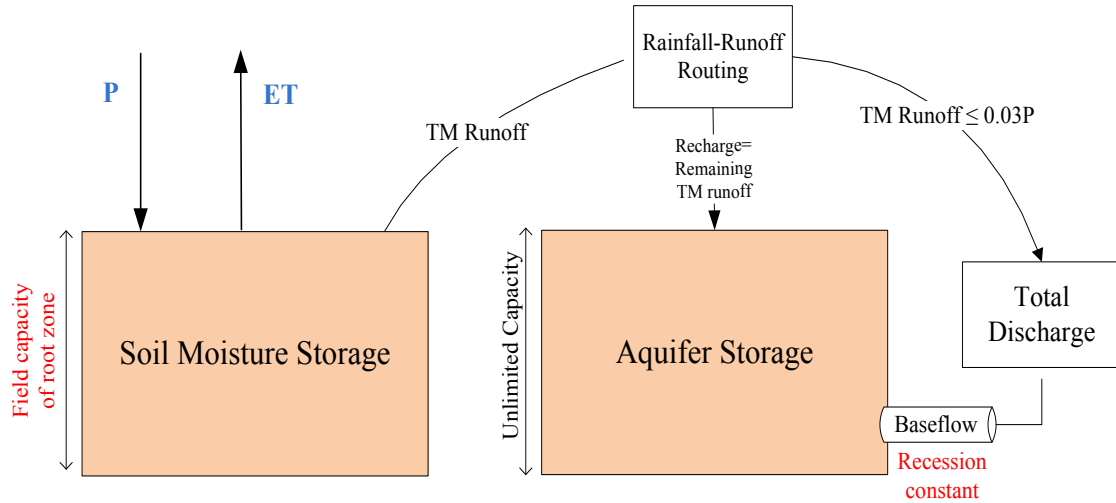
Figure 3.4 Model 1 conceptualization (parameters are in red)

yearly constant, will instantly runoff rather than enter aquifer storage. Any TMWB runoff in excess of that value is then routed to aquifer storage.

The equations, after TMWB runoff is generated, begin with the runoff constant function as follows:

$$\text{If } R_1 \leq P \cdot RC, \text{then } Q_1 = R_1 \tag{6}$$

$$\text{If } R_1 > P \cdot RC, \text{then } Q_1 = P \cdot RC, R_1 - Q_1 = R_2 \tag{7}$$

Any excess runoff then recharges the aquifer, accumulating with the previous month's final storage:

$$S_I = R_2 + S_{F(t-1)} \tag{8}$$

The aquifer storage then drains as a function of the base flow recession constant:

$$S_I \cdot k = Q_2 \tag{9}$$

with the remainder being the initial aquifer storage for the next month:

$$S_I - Q_2 = S_F \tag{10}$$

The sum of immediate discharge and baseflow recession is total discharge:

$$Q_1 + Q_2 = Q_T \tag{11}$$

where:

20

R_1 = Thornthwaite-Mather runoff (mm)

P = Annual precipitation (mm)

RC = Runoff constant (%)

Q_1 = Instant discharge (mm)

R_2 = Aquifer recharge (mm)

S_I = Initial aquifer storage (mm)

S_F = Final aquifer storage (mm)

k = Baseflow recession constant (1/mo)

Q_2 = Baseflow discharge (mm)

Q_T = Total discharge (mm)

Model 1 has two parameters to calibrate, the *TMWB soil$_{max}$* and k. The *RC* function is constant is discussed further in Chapter 5.

3.3.2 Model 2

Figure 3.5 illustrates a second model that was constructed based on a different conceptualization of the catchment system. Removing the *RC* function, all TMWB runoff is routed to aquifer storage. Aquifer storage is allowed to fill until a 'maximum' is reached, as determined by the S_{max} parameter, and then the excess runs off. Aquifer storage is again drained by baseflow at a rate determined by k.

The equations for Model 2, after initial TMWB runoff, are as follows:

$$S_{F(t-1)} + R_1 = S_I \tag{12}$$

When summed, if TMWB runoff and previous aquifer storage exceeds total aquifer storage capacity then the difference becomes discharge:

$$IF\ S_I > S_{max}, then\ S_I - S_{max} = Q_1 \tag{13}$$

The remaining storage, which if the above condition is true, will be equal to S_{max} and is then drained by the recession constant:

$$S_J \cdot k = Q_2 \tag{14}$$
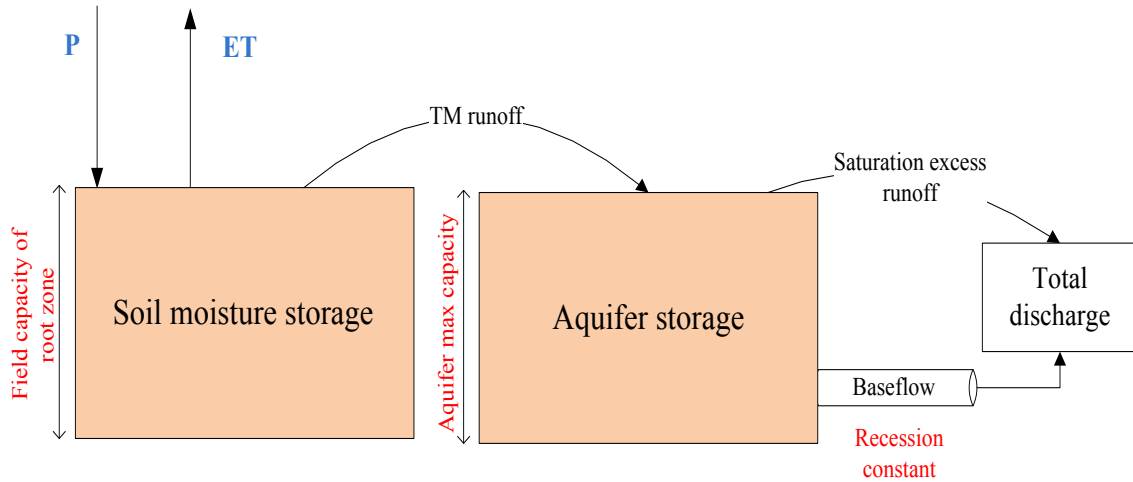
Figure 3.5 Model 2 conceptualization (parameters are in red)

Final aquifer storage, which then carries over to the next month, is what remains after the baseflow discharge is accounted for:

$$S_J - Q_2 = S_F \qquad (15)$$

Total discharge is equal to saturation excess discharge and baseflow discharge:

$$Q_2 + Q_1 = Q_T \qquad (16)$$

where:

   R_1 = Thornthwaite-Mather runoff (mm)

   S_{max} = Aquifer storage capacity (mm)

   S_I = Initial aquifer storage (mm)

   S_J = Intermediate aquifer storage (mm)

   S_F = Final aquifer storage (mm)

This model has three parameters to calibrate: *TMWB soil$_{max}$*, *S$_{max}$* and *k*. Spreadsheets of both models and the original TMWB are found in the accompanying CD.

3.3.3   Model Calibration

Modeled monthly discharges were calibrated to maximize the Nash-Sutcliffe efficiency (*E*). This 'goodness-of-fit' measure was first proposed by Nash and Sutcliffe (1970) and has since been used extensively in hydrologic modeling to assess model performance. It is given as (Krause et al. 2005):

$$E = 1 - \frac{\sum_{i=1}^{N}(Q_i - Q_m)^2}{\sum_{i=1}^{N}(Q_i - \overline{Q})^2} \qquad (17)$$

where:

    Q_i = observed flow (mm)

    $\overline{Q}$ = mean flow (mm)

    Q_m = modeled flow (mm)

E is a measure of the squared difference of observed and modeled values divided by the variance in the observed data (Nash and Sutcliffe 1970). Although E has been shown to over emphasize large flow volumes, this research focuses on low flows in the dry season and, since they exhibit small variations over time, this efficiency statistic is considered reasonable (Legates and McCabe Jr. 1999).

Legates and McCabe Jr. (1999) suggest complementing Nash-Sutcliffe efficiency with absolute measures of model performance. Therefore, calibration results include modeled dry-season discharge means, standard deviations, and square root of the mean standard error (*RMSE*) given as:

$$RMSE = \sqrt{N^{-1}\sum_{i=1}^{N}(Q_i - Q_m)^2} \qquad (18)$$

and mean absolute error (MAE) denoted by:

$$MAE = N^{-1}\sum_{i=1}^{N}|Q_i - Q_m| \qquad (19)$$

Since the discharge dataset is short, the models are not validated as is customary in hydrological modeling. Instead, a cross-validation technique that divides the discharge record into sections for calibration and validation is used. For example, the dry-season discharge is calibrated to 2005-2008 and validated in 2009, and the *RMSE* is reported for the calibration and validation period. This is repeated for all possible permutations of consecutive years of discharge.

3.4   Simulating Climate Changes

A number of methods exist which incorporate predicted climatic data into hydrologic models (Xu 1999), and many modelers are using GCM results to simulate future hydrologic changes (Varis et al. 2004). However, some modelers do not use the GCM outputs because they do not produce reliable estimates of future climatic conditions at the necessary scale for hydrologic models (Kilsby et al. 1998). These modelers instead alter historical data within certain conditions, comparing the modeled results to the historic simulations. This technique is used to create climate scenarios for model testing, since GCM outputs for East Africa are uncertain and inconclusive.

There are two main shortcomings with this method: 1) it assumes that the distribution of wet years and dry years remains constant through time (Kilsby et al. 1998), and 2) it presumes that physical conditions and processes within the catchment itself, such as vegetation and land use, will continue to behave the same (Beven 2006). This research does not attempt to overcome these disadvantages but acknowledges the inherent uncertainty in them. Rather than considering the results of these simulations as predictions, it is appropriate to view them as indicators of hydrologic system sensitivity to climatic factors, all else assumed constant (Xu and Singh 2004).

The sensitivities of both models to climate changes were tested by perturbing the historic climate dataset to decrease total annual precipitation, increase temperature, reduce wet season length, and alter seasonal rainfall distribution. Table 3.1 summarizes the climate scenarios tested. To simulate a reduction in wet season length, precipitation is zeroed in the final wet-season months. First May, then April and May, and then March through May precipitation is removed to see how the model responds. Rainfall distribution is altered by adding precipitation in 60 mm increments to the beginning of the wet season (November-January) and subtracting that amount from March-May precipitation. The 60 mm change is spread evenly across the months at 20 mm/mo and precipitation can never be below zero.

The scenario results are compared to the calibrated model based on relative change in aquifer storage at the end of May. Since dry-season discharge is a function of storage and May is typically the last month with storage recharge, relative changes in aquifer conditions and dry-season discharge due to climate alterations should be reflected in aquifer storage at the end of May.

Table 3.1

Perturbed climate scenarios - P is precipitation, T is temperature, Ws_b is the beginning of the wet season (November to January), and Ws_e is the end (March to May)

Scenario #	Change		Scenario #	Change
1	P -10%		11	P -20%, T +2°
2	P -20%		12	P -10%, T +3°
3	P -30%		13	P -20%, T +3°
4	T +1°		14	May (P=0)
5	T +2°		15	April, May (P=0)
6	T +3°		16	March, April, May (P=0)
7	T +4°		17	Ws_b (P +60 mm), Ws_e (P -60 mm)
8	P -10%, T +1°		18	Ws_b (P +120 mm), Ws_e (P -120 mm)
9	P -20%, T +1°		19	Ws_b (P +180 mm), Ws_e (P -180 mm)
10	P -10%, T +2°			

4   DATA

4.1 Temperature

Monthly temperature information was collected for an observation station about 35 km west of the Jandu catchment called Basotu Plains (4 22' 15" S, 35 05' 30" E, 1671 mamsl) (AWMP 2000). The average elevation of Jandu catchment is 2646 m (a 1000 m difference from Basotu Plains), so temperatures were corrected following Bedient et al. (2002) with an adiabatic lapse rate of 6.5 °C/1000 m (see Table 4.1).

4.2 Precipitation

The monthly precipitation record from 1984-2010 is summarized in Appendix 8.6 and is also in the accompanying CD. Since data for 2003 were absent, the mean monthly precipitation values of the remaining years were used to complete the record. Data was classified in hydrologic years, as September through August, because of the clear distinction between wet and dry seasons (see Figure 4.1). Regional precipitation does not exhibit a bimodal distribution, with a 'long rains' and 'short rains', common to East Africa. Rather, it is well distributed from November through May, which henceforth is referred to as the 'wet season'.

Mean rain-year precipitation is 705 mm, with a standard deviation of 307 mm. Maximum rain-year precipitation was 1868 mm in 1997-98, an El Niño year, while the minimum was only 60 mm 2 years later during a La Niña event. Inter-seasonal variation is also high: January through March has experienced rainfall as much as 300% of the mean, while at other times experiencing none. Figure 4.2 depicts the inter-annual variability as precipitation anomalies, corroborating previous observations that East African rainfall is extremely variable (Kabanda and Jury 1999).

Table 4.1
Mean monthly temperatures (°C) for Basotu Station and Jandu corrected temperatures
(Source: AWMP 2000)

	Jan	Feb	Mar	Apr	May	Jun	Jul	Aug	Sep	Oct	Nov	Dec
Basotu	20	20	20	20	19	20	18	19	20	21	22	22
Jandu	14	14	14	14	13	14	12	13	14	15	15	15
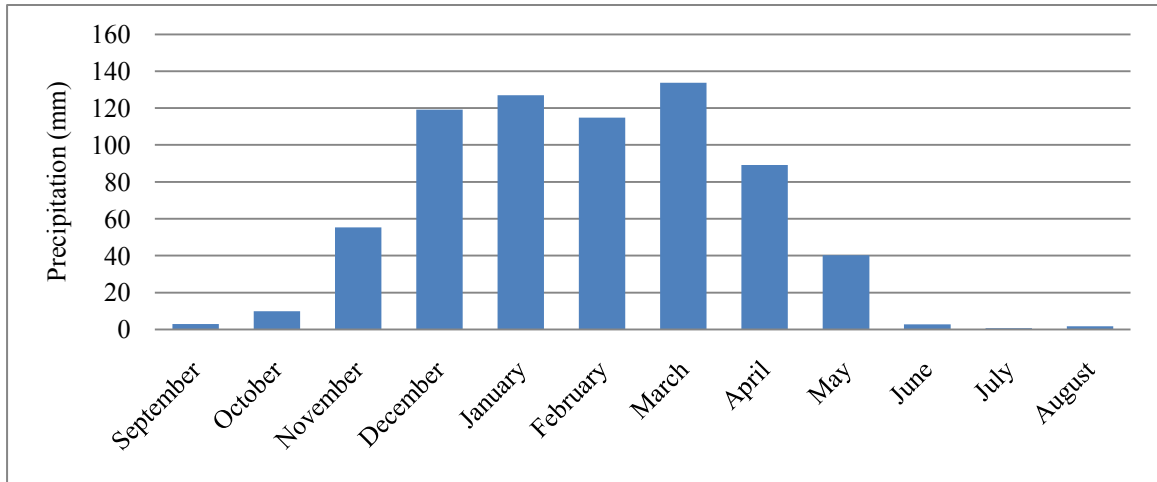
Figure 4.1 Katesh mean monthly precipitation (1984-2010) (Source: AWMP, 2000)

4.3 Discharge

Daily discharge data for 2004-2010 were obtained from the weir caretaker (Oreste 2010). It is aggregated to monthly discharges for analysis and the entire data set is compiled in Appendix 8.7 and the accompanying CD. The data exhibits the same distinction between the wet and dry seasons as the precipitation data and, therefore, is also analyzed in rain years (see Figure 4.3). An El Niño event in 2007-2008 dominates the statistical analysis of this short record.

Mean annual runoff was 11.8 Lps in 2004-2010, with a range of 7.9-20.0 Lps. Mean wet-season discharge was 15.0 Lps, with a high in 1997 of 27.2 Lps. Mean dry-season discharge was 7.5 Lps, with a low in 2007 of 5.1 Lps. October, which is typically the last month of the dry season, consistently has the lowest discharge values.
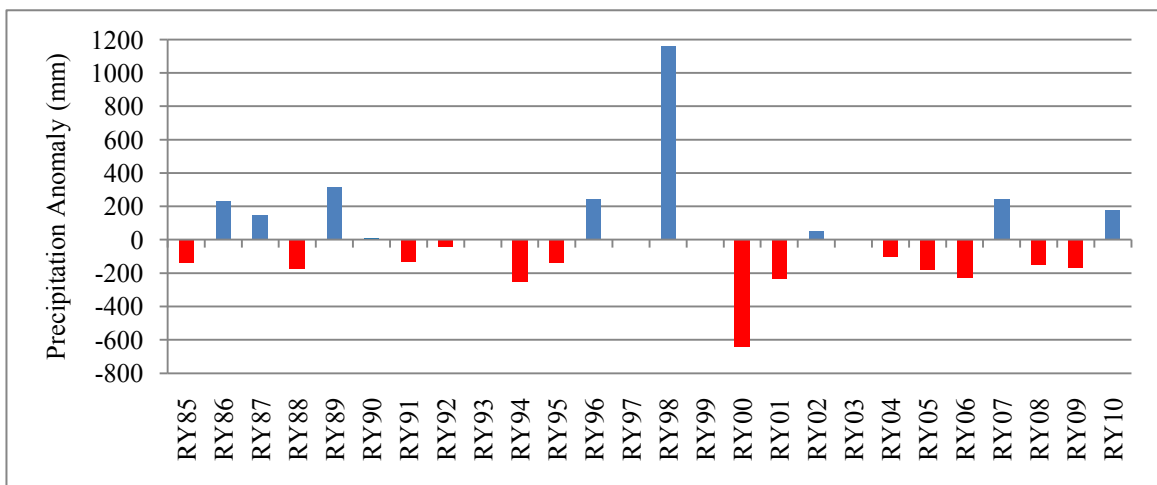
Figure 4.2 Annual precipitation as deviation from the mean. Blue is positive deviation and red negative, *RY* is rain-year (Source: AWMP, 2000)

27
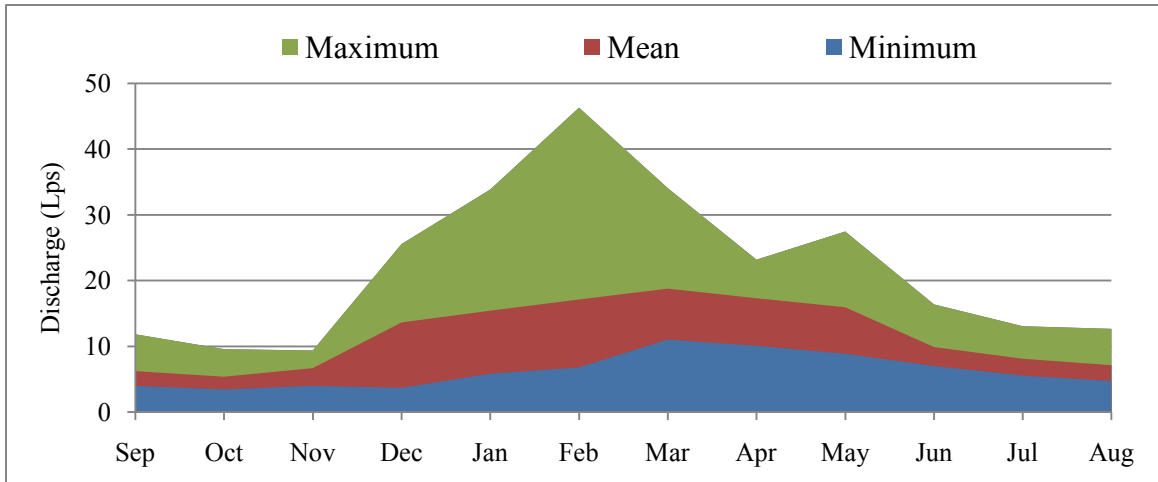
Figure 4.3 Minimum, maximum, and mean Jandu discharge (2004-2010) (Source: Oreste, 2010)

Mean October discharge for the record is 5.4 Lps, with a low of 3.4 Lps measured in 2010. Discharge is converted to millimeters for analysis by dividing by catchment area. Many discrepancies are apparent when the discharge hydrograph and precipitation are plotted over time (see Figure 4.4), increasing the uncertainty in using Katesh precipitation data to represent rainfall at Jandu catchment.
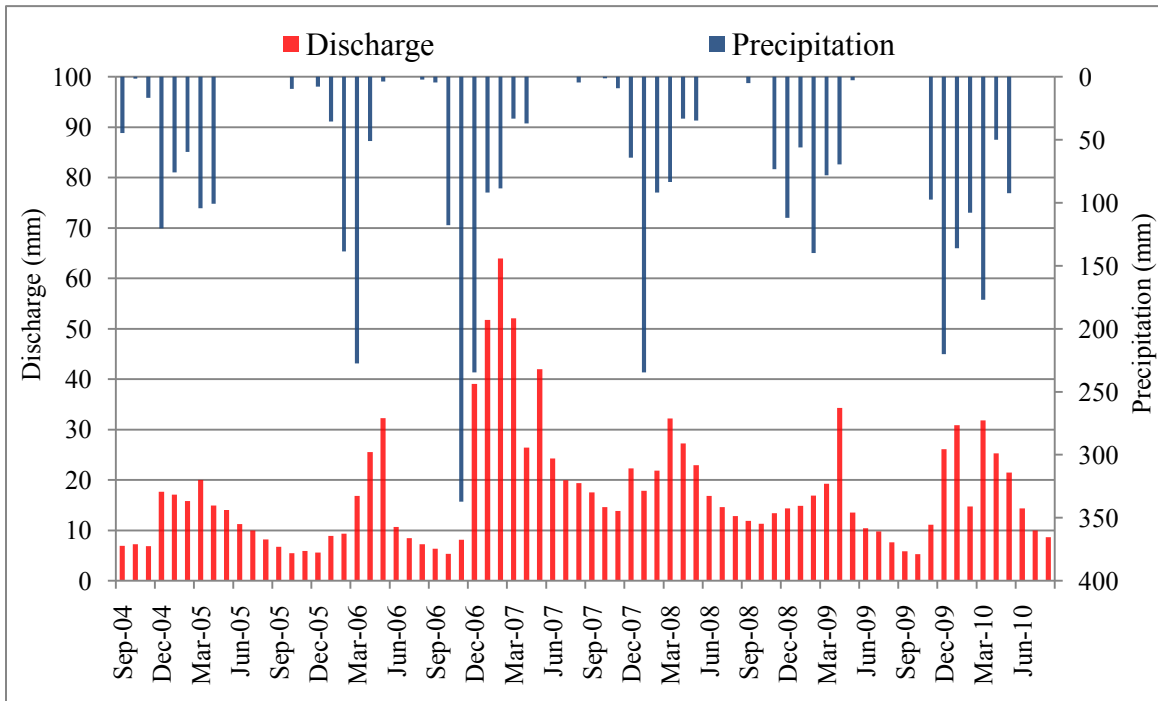
Figure 4.4 Jandu discharge and Katesh precipitation (2004-2010). Note that the scales are different (Sources: AWMP 2000; Oreste 2010)

5   RESULTS & DISCUSSION

5.1   Water Quality Parameters

Analysis of Jandu reservoir water quality samples, summarized in Table 5.1, demonstrates a meteorically recharged, shallow aquifer system. pH measurements are slightly basic, likely reflecting leaching from the calcareous material. An anomalous low value on February 25 was recorded immediately after a rainfall event, so it is thought to reflect high concentrations of overland flow and less groundwater. From March to September, the pH changed very little, suggesting that hydrogen ion activity has reached equilibrium with the aquifer rocks.

Temperature remains relatively constant throughout the wet season, decreases into the dry season, and then increases slightly in September. This trend is seen in ambient air temperature as well. Measurements were taken at varying times of the day, and because the sampled water has been surface water for an unknown time, air surface temperature affects water temperature to an unknown degree. However, the water is never warmer than surface temperature, so geothermal heating is assumed minimal. The cooler water probably reflects the higher altitudes at which it was recharged.

Electrical conductivity dropped significantly in April, probably due to sampling of a runoff event, and increased slightly as the dry season progressed. This is typical for systems with strong dry seasons in which recharge ceases and dissolution of the aquifer media by groundwater occurs without dilution. The purity of the water suggests that recharge to the system is dominated by rainfall and that groundwater residence time is relatively short.

Table 5.1
Jandu stream water quality and geochemistry measurements for 2010

Date	pH	Temp (°C)	EC (μs)	Hardness ($CaCO_3$) (mg/L)	Na^+ (mg/L)	Fl^- (mg/L)	SO^{2-} (mg/L)
25-Feb	8.2	16.9	271				
12-Mar	8.5	16.9	257				
2-Apr	8.5	15.9	236				
31-May	8.4	15.4	269	95	17	2.6	7
5-Jul	8.5	13.1	274				
2-Aug	8.4	11.5	277				
4-Sep	8.5	12.4	281	98	19	2.6	7

The lab reports, which include hardness, alkalinity, and basic anions and cations, are reported in Appendix 8.8. Both samples are characterized by low concentrations of anions and cations and almost no nitrites or nitrates. With an average hardness (as $CaCO_3$) of 96 mg/L, the samples can be considered moderately hard (Fetter 2001). This is not surprising considering the dominant geology is nephelinitic and calcareous strata, which both readily leach calcium carbonate.

Fluoride concentrations in both samples were 2.6 mg/L. This is higher than the World Health Organization guideline of 1.5 mg/L, but below the Tanzania standard of 4.0 mg/L. Concentrations of this level may lead to dental fluorosis: however, much higher concentrations are necessary to cause more serious, adverse effects (WHO 2003). Fluoride has been found in groundwater throughout the Gregory Rift Valley and is thought to originate from the volcanic complexes of the region (Ghiglieri et al. 2009).

5.2   Recession Analysis

Jandu discharge data was analyzed, a baseflow recession curve plotted, and an average monthly recession constant calculated for the dry seasons in 2004 through 2010. When log-discharge is plotted as a function of time, the trend line is near-straight (R^2=0.95-0.99), suggesting the reservoir acts as a linear store and can be characterized with Eqs. (3) and (4) (Tallaksen 1995). A single, linear storage-discharge relationship for an aquifer assumes that the recession curve is constant from year to year (Hall 1968). This assumption is not true for Jandu (see Table 5.2), so the recession constants for each year are averaged together to derive a recession constant for model parameterization.

The recession constants range from 0.100 to 0.189/mo with a mean of 0.151/mo, but the recession rate itself ($\Delta Q/\Delta t$) is quite consistent except for 2007, the high-precipitation El Niño year. These recession constants are similar to constants obtained by Zecharias and Brutsaert (1988) in mountainous watersheds, and slightly higher than those calculated by Brandes et al. (2005) of 0.148/mo.

The derived recession constant seems consistent with Jandu's steep slopes and drainage patterns, even though there are no recession constants for other local watersheds to compare it with. This assertion comes from the correlations between recession constant, catchment slope, and drainage density made by Zecharias and Brutsaert (1988) and Brandes et al. (2005). Unfortunately, no empirical estimation of drainage density is available, nor are there other catchments with which to compare Jandu's recession constant. Thus, no definitive conclusions can be drawn from the recession analysis, other than that the recession constant is within reasonable agreement with other steep, mountainous catchments, and the reservoir behaves linearly.

Table 5.2
Monthly recession constants (k) for dry seasons 2005 through 2009

Year	$\Delta Q/\Delta t$ (mm/mo^2)	k (1/mo)
2005	1.44	0.182
2006	1.33	0.168
2007	2.40	0.114
2008	1.38	0.100
2009	1.30	0.189

5.3 Water Balance Model Calibrations

Table 5.3 presents the results of model calibration. Nash-Sutcliffe efficiencies (E) were both high, but Model 2 resulted in the best fit to the observed dry-season data (+0.05 mm higher than Model 1) at 0.91 mm. MAE was 1.1 mm for both, but RMSE was 0.3 mm higher for Model 1 at 1.6 mm than Model 2. Mean dry-season discharge was reproduced within 0.1 mm in both models, suggesting that both accurately represent mean dry-season flows. However, observed year-to-year discharges were often different from modeled discharges (see Figure 5.1).

The models produce very similar dry-season discharges, but Model 1 is much better at replicating wet-season discharge. This is due to the incorporation of the runoff constant function, which was calculated by evaluating the relationship between annual catchment rainfall and monthly runoff. The calculated mean wet-season discharges are, on average, 3.1% of annual precipitation. This correlates to the lower end of average runoff

Table 5.3
Model calibration results - E is Nash-Sutcliffe efficiency coefficient, MAE is mean absolute error, RMSE is root mean square error, k is recession constant, *TMWB soil$_{max}$* is Thornthwaite-Mather maximum soil moisture storage, S_{max} is maximum aquifer storage, Mean Ds Q is mean dry-season discharge, May S is mean May storage. Observed values were calculated from the discharge record 2004-2009.

	Goodness of Fit			Parameters			Outputs	
		MAE	RMSE		TMWB soil$_{max}$	S_{max}	Mean Ds Q	May S
	E	(mm)	(mm)	k (1/mo)	(mm)	(mm)	(mm)	(mm)
Model 1	0.86	1.1	1.6	0.052	95		9.8	314
Model 2	0.91	1.1	1.3	0.062	138	392	9.8	246
Observed				0.151			9.7	
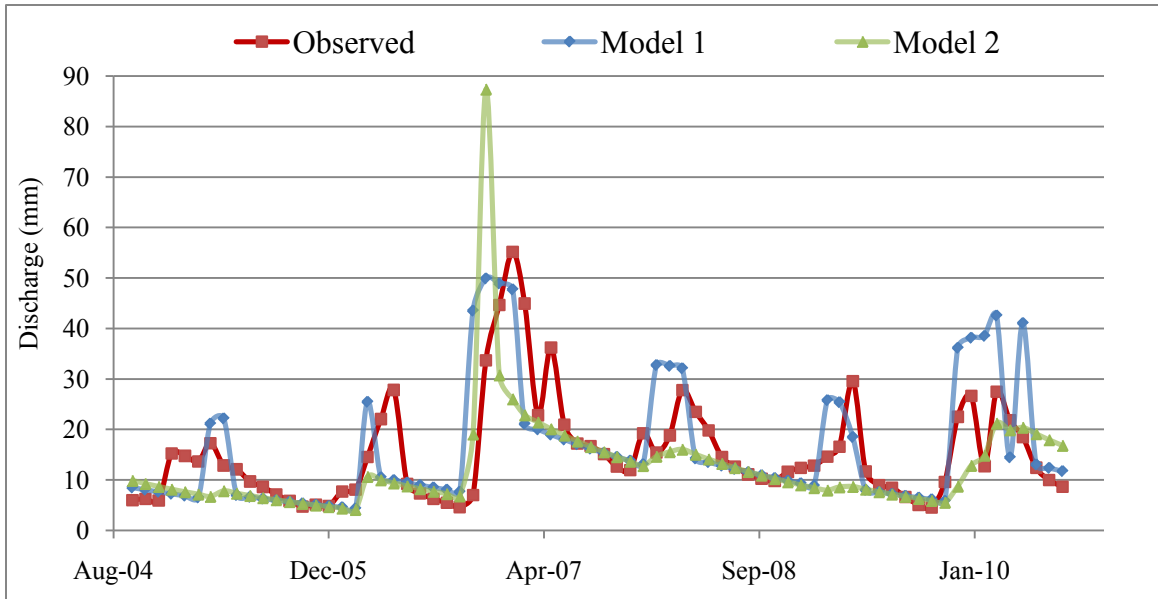
Figure 5.1 Dry-season discharge for observed data, Model 1, and Model 2 (2004-2009)

percentages calculated by JICA (2008) for the area. However, uncertainty in both the spatial accuracy of the precipitation data and temporal resolution of the discharge data makes the accuracy of the rainfall-runoff relationship uncertain. This is because the daily observed discharge measurements probably do not accurately capture peak runoff events (due to catchment size and sampling rate), and accumulated monthly totals likely underestimate actual discharge. Therefore, since error in the runoff constant could be great and Model 2 fits the dry-season data better, the runoff constant and reproduction of wet-season discharges in Model 1 are deemed unnecessary components.

Model 2 does not allow precipitation to instantly run off and wet-season discharge is rarely comparable to the observed data. This model routes all initial runoff to aquifer storage first, conceptually akin to an interflow and baseflow component. So, the soil has to be completely saturated before runoff can occur, and the 'saturation excess' that does discharge can be thought of as quick flow and interflow. Less water leaves the system than in Model 1. Yet, the mean dry-season discharges are accurately reproduced, suggesting that more evapotranspiration occurs in Model 2 than in Model 1.

Figure 5.3 shows the total annual evapotranspiration produced by the models, which is very similar: 435 mm for Model 1 and 469 mm for Model 2. Model 2 is consistently higher due to the greater TMWB $soil_{max}$ value. Annual evapotranspiration exhibits minimal variance throughout the record, in the range of 400 to 500 mm, even though the precipitation record has great variance. This suggests that evapotranspiration is limited
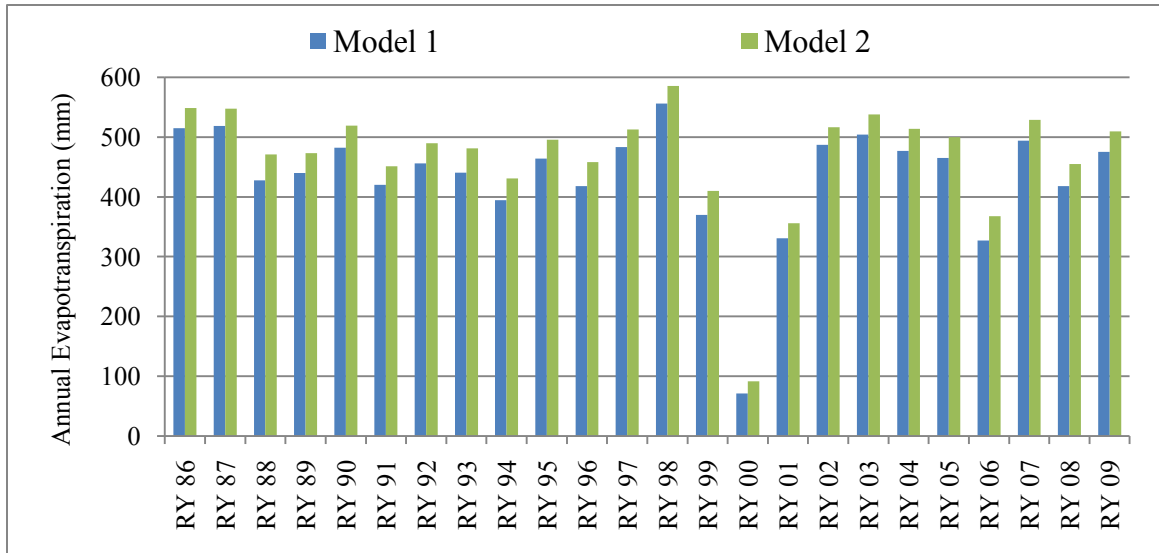
Figure 5.2 Modeled annual evapotranspiration, *RY* is rain-year

by factors other than total precipitation. Potential evapotranspiration is almost always exceeded in the wet season, and as it is calculated from the Hamon method, temperature is the limiting factor. In the dry season, though, evapotranspiration is limited by TMWB soil moisture capacity, which is quickly depleted and does not allow further evaporative losses.

Although the Jandu mean-monthly recession constant was calculated to be 0.151/mo, model calibration yielded much lower values: 0.052 for Model 1 and 0.062 for Model 2. This could be due to the models' consistent underestimating of the storage and discharge in the first months of the dry season. Figure 5.4 displays an example of modeled and
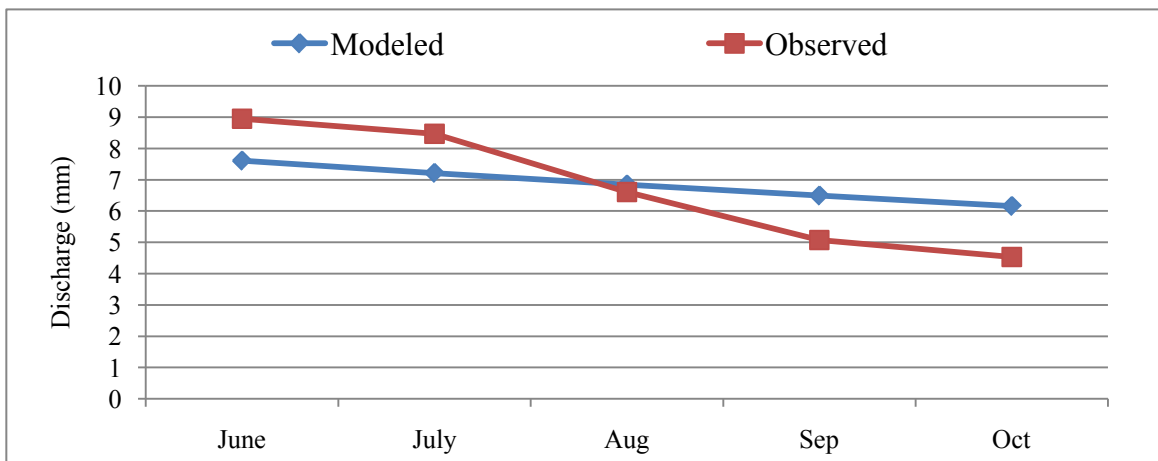
Figure 5.3 Dry season 2009 - Model 1 discharge and observed discharge

observed flow from the 2009 dry season and how using a lower recession constant counteracts the models' temporal inability to initiate the dry season correctly. Discharge, controlled only by the recession constant, begins earlier in the year, but it recedes at a slower rate than the observed data. This effectively reproduces the *average* discharge rather than the actual discharge, thus giving high model efficiency values.

The results from the cross validation are reported in Table 5.4. Calibration scenarios 5 and 9 have only one year of calibration and exhibit the lowest calibration RMSE (C-RMSE) for both models, but validation RMSE (V-RMSE) is great. V-RMSE for both models is low (1.2-1.4 mm) for scenarios 2 and 3, which utilize three and four year calibration periods, respectively. Scenario 3 has the lowest V-RMSE for both models, demonstrating that the models only need to be calibrated to data from 2005-2007 in order to accurately reproduce observed discharges for 2008-2009. When calibrated for 2007-2009, the V-RMSE for 2005-2006 were between 1.7 and 3.8 mm. More research is necessary in different catchments, but the cross validation suggests that TMWB models can be parameterized and calibrated to reproduce dry-season discharges with short (3-4 year) discharge records.

The relationship between June and October discharge for the observed data is shown in Figure 5.4. The trend line ($R^2 = 0.93$) clearly shows a linear trend with October discharge equaling about 60% of June discharge. The recession constants that were calibrated for the models, though, produced October discharges that were roughly 80% of June discharge. With this relationship, water managers for the catchment can make predictions of October discharge from June discharge, thereby giving some warning of potential dry-season water scarcity.

Table 5.4

Results of model cross validation – *C* is calibration period, *V* is validation period, *RMSE* is root mean square error. Calibration scenario 1 is of models calibrated to entire dataset.

Calibration Scenario	2005	2006	2007	2008	2009	Model 1		Model 2	
						C-RMSE (mm)	V-RMSE (mm)	C-RMSE (mm)	V-RMSE (mm)
1	C	C	C	C	C	1.6		1.3	
2	C	C	C	C	V	1.7	1.3	1.4	1.4
3	C	C	C	V	V	1.9	1.2	1.5	1.3
4	C	C	V	V	V	1.5	3.8	1.3	1.5
5	C	V	V	V	V	0.2	5.4	0.2	3.8
6	V	C	C	C	C	1.5	2.3	1.3	2.0
7	V	V	C	C	C	1.7	3.8	1.3	1.7
8	V	V	V	C	C	0.7	3.4	0.6	4.4
9	V	V	V	V	C	0.5	5.4	0.4	4.0

The current estimate of population served by the Jandu catchment is 4,000, and if we assume the World Health Organization WHO water consumption standard of 20 Lcd (liters per capita per day), the amount of water necessary to supply all demand is 80,000 L d^{-1}. Given an estimated 50% system inefficiency, the demand is 160,000 L d^{-1}. This is equivalent to a discharge of 0.08 mm. This discharge would be reached in October if June discharge was 0.14 mm. This is unlikely, even with intense changes in climate, but the population that Jandu serves will undoubtedly increase. More research is necessary to determine the accuracy of the served population and its growth rate, but water resource managers can still use this relationship to forecast dry-season discharge.

Model 1 incorporated two new parameters, a runoff constant and an aquifer storage function, to the original TMWB model, and discharges were very accurately reproduced. The removal of the runoff constant and addition of an aquifer capacity parameter for Model 2 yielded a slight increase in accuracy. Mean dry-season discharges are well reproduced by both models, suggesting that the TMWB model can successfully be adapted with minimal parameterization and applied to small, semi-arid catchments.

Some shortcomings and uncertainties should also be elucidated. Precipitation during the discharge calibration period ranged between 476 mm and 949 mm, so discharge volumes modeled in years with precipitation out of that range must be viewed with caution. The precipitation gage from which records were taken is about 8 km away, and on the another side of the mountain, so whether or not measurements accurately portray rainfall within the catchment is unknown. Comparison of the discharge and precipitation data did show discrepancies. Ideally, the models would be calibrated to one long period of observed
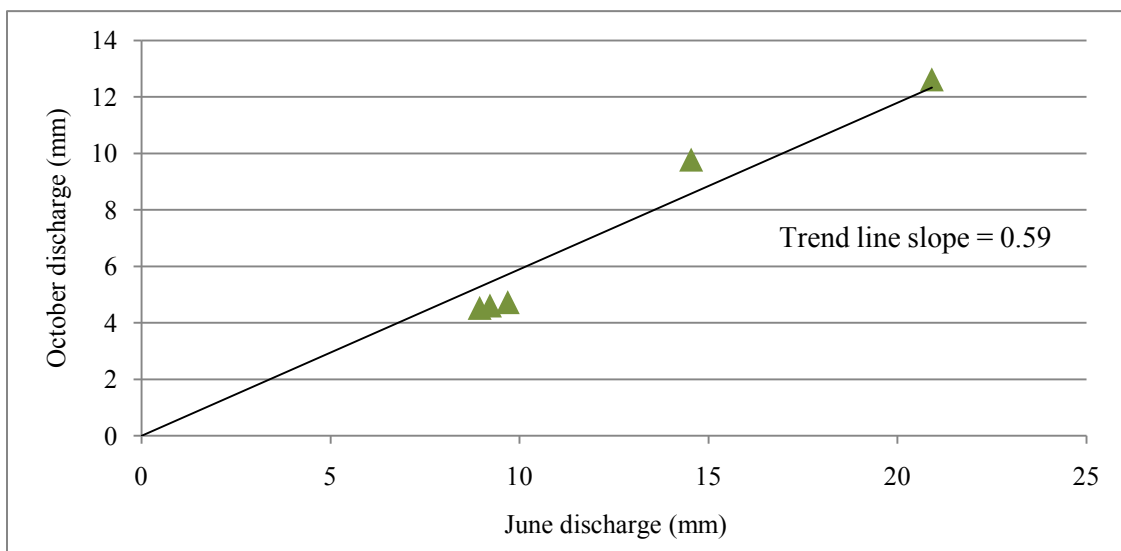
Figure 5.4 June and October discharge (2004-2009)

data and then validated to another period, but only one reliable period of discharge data is available, so the models are not properly validated. The cross validation method would need to be further tested before considered an actual model validation. The only confident assertion that can be made is that these models accurately reproduce discharges during the calibration period and conditions of the dry seasons in 2004 through 2009.

5.4   Climate Scenarios

Table 5.5 presents the results from the climate scenario simulations in terms of percent change in May mean aquifer storage. Both models yield similar results for the given scenarios, so henceforth the results are discussed as averages of the two. The similarity is not surprising considering that both rely on the TMWB to produce initial runoff values.

The models were more sensitive to changes in precipitation than temperature, but changes in both produced significant changes in relative storage. According to the models, the effects of a 10% reduction in precipitation are approximately equal to the

Table 5.5

Climate scenario results as percent changes in May mean aquifer storage (%ΔS)

Scenario		Model 1 %ΔS	Model 2 %ΔS	Average %ΔS
ΔP	-10%	-25	-19	-22
	-20%	-48	-42	-45
	-30%	-67	-64	-66
ΔT	+1°	-8	-7	-8
	+2°	-16	-13	-15
	+3°	-23	-19	-21
	+4°	-30	-26	-28
T+1, P-10%		-32	-25	-29
T+1, P-20%		-53	-48	-51
T+2, P-10%		-38	-32	-35
T+2, P-20%		-58	-55	-57
T+3, P-10%		-44	-39	-42
T+3, P-20%		-63	-60	-62
T+4, P-10%		-49	-46	-48
T+4, P-20%		-67	-65	-66
May P=0		0	-4	-2
Apr & May P=0		-12	-18	-15
March, April, May P=0		-42	-54	-48
Ws_b (P +60 mm), Ws_e (P -60 mm)		1	0	1
Ws_b (P +120 mm), Ws_e (P -120 mm)		8	3	6
Ws_b (P +180 mm), Ws_e (P -180 mm)		20	9	15

effects of a 3 °C increase in temperature. For every 10% reduction in precipitation, storage reductions of 22% occur, giving a maximum change of -66% for a 30% decrease in precipitation. Relative changes in storage were nearly double the relative changes in annual precipitation. This suggests that even small changes in mean precipitation can have large effects on catchment discharge.

Temperature changes also had significant effects: a 1 °C increase (7.5% of the mean annual temperature of 13.5 °C) led to an 8% storage reduction, and a 4 ºC increase reduced storage by 28%. This suggests that changes in temperature, and thus evapotranspiration will have significant impacts on aquifer storage and groundwater discharge. However, the TMWB model uses a simplistic method of calculating evapotranspiration and soil moisture storage, and does not account for other factors including the effects that atmospheric CO_2 increases and temperature changes may induce in vegetation growth, relative humidity, and soil moisture storage processes in the catchment.

Scenarios that combined increasing temperature and decreasing annual precipitation produced the largest storage reductions. Storage decline approached 30% for the most moderate scenario of +1 °C and -10% P, whereas the most extreme scenario of +4 °C and -20% P generated storage reductions of 66%. This appears to show that both models approach a leveling-off point as the climate continues to change. For example, the decline of 30% experienced in the most moderate scenario is equal to the sum of the reductions from the individual scenarios of increasing temperature 1 °C and decreasing precipitation 10%. However, the most extreme scenario results are 7% less than they would be if the reductions are summed from individual rainfall and temperature changes. These reductions are about 10% greater than reductions found by Jiang et al. (2007) for a large basin, but the magnitude of change between simulations is similar.

When wet-season length was adjusted by zeroing precipitation in May, then April and March, the change in storage was -2%, -15%, and -48%, respectively. This suggests that March precipitation contributes about 33% of dry-season storage, while precipitation in April and May cumulatively only contributes 15%. The precipitation record was analyzed to determine relative contributions of March, April, and May precipitation to the cumulative total: March precipitation is 19% of total annual precipitation, April is 13%, and May is 6%. Together, March through May account for 38% of total rain-year precipitation, so it is not surprising that removing this amount of total precipitation has such a strong impact on May aquifer storage.

Scenarios that altered seasonal distribution of rainfall generated increases in May mean aquifer storage values. Reducing precipitation in March to May and increasing it in November to January, increased mean May storage by 1 mm, 6 mm, and 15 mm, for

changes of 60 mm, 120 mm, and 180 mm respectively. This demonstrates that either the models or this method of altering rainfall distribution is inadequate for accurate forecasts. The low recession rate allows aquifer storage to fill up, regardless of when, and slowly release that water throughout the year. Thus, the models' May storage is overestimated, and the large aquifer storage capacity allows the water lost from the end of the wet season to be stored in the beginning. Since precipitation for any month can never go below zero and the end of the wet season is often characterized by low rainfall, this method sometimes increases total annual precipitation. If the distribution was not evenly spread over the months, but distributed to have a net-zero effect on total precipitation, this shortcoming could be addressed. These models, when given these scenarios and tested with this method, suggest than changes in rainfall distribution will have an impact on dry-season storage, however, more thorough evaluation is necessary before more certain quantifications can be made.

6   CONCLUSION

A small, spring-dominated catchment on Mt. Hanang, Tanzania was analyzed to determine general aquifer characteristics and hydrologic functioning. Geochemical analysis, recession flow analysis, and water balance models were applied to characterize the system.

The geochemistry shows a meteorically-recharged, shallow aquifer system with quickly circulating groundwater. Recession flow varied from year to year, but an average monthly constant of 0.151/mo was calculated for the 2004-2009 discharge dataset. This is consistent with data from other mountain catchments.

Two models were developed from the Thornthwaite-Mather Water Balance model that accurately reproduced observed dry-season discharges. Information obtained from analysis of precipitation data and discharge hydrographs, the runoff constant and recession constant, were successfully used to improve model performance. For the calculated recession constant to be effectively applied, a model must accurately reproduce wet-season discharge and storage values as well.

Once the models were calibrated, the historic climate data was perturbed to reflect increasing temperatures and decreasing precipitation. Modeled storage values from these scenarios show that small climatic changes could have large hydrologic consequences, but the amounts determined herein are relative and cannot be offered as quantitative forecasts. The study confirms previous findings that climate change will significantly impact hydrologic systems, and that water balance models, modified to local conditions and calibrated to historic data, are tools that offer a simple and accurate method of assessing hydrologic conditions and outputs.

7   FUTURE WORK

There is much that could be done to improve and enhance a project like this one. To ensure model inputs are accurate, catchment precipitation gages and thermometers could be deployed. Soil samples could be analyzed and cores drilled to better classify watershed geology and assist with model parameterization. If more discharge data were available, the models could be further validated and finely tuned. The geochemical and flow data for Jandu stream could be contrasted to that of other Hanang springs and streams. If those springs and streams are found to behave similarly to Jandu, and hence have similar catchment properties and storage structures, spot measurements of discharge could perhaps allow the estimation of complete discharge time series. Then their low flows could be assessed and modeled and relative climate change forecasts extrapolated.

Recession analysis has potential to help determine aquifer characteristics in sparsely gauged basins. Further analysis of recession data would yield more information about aquifer parameters, flow components, and catchment characteristics. This information could be compared for multiple basins and then cross-correlated to physical watershed parameters like drainage density, slope, and hydraulic conductivity. If regional patterns became apparent, ungauged basins in the region could potentially be analyzed with spot discharge measurements.

The water balance models have shown their ability to reproduce historical dry season flows, but it is unknown if they have the ability to forecast future discharges. Analysis like that presented here could be carried out for any catchment, and then that catchment could be monitored in the future and changes in discharges compared to climate changes. The agreement between the model predictions and actual discharges could be assessed and more certainty applied to future forecasts from such models.

REFERENCE LIST

Abram NJ, Gagan MK, Liu Z, Hantoro WS, McCulloch MT, Suwargadi BW. 2007. Seasonal characteristics of the Indian Ocean Dipole during the Holocene epoch. Nature. 445(7125):299-302.

Alley WM. 1984. On the treatment of evapotranspiration, soil moisture accounting, and aquifer recharge in monthly water balance models. Water Resources Research. 20(8):1137–1149.

Arnell NW. 1992. Factors controlling the effects of climate change on river flow regimes in a humid temperate environment. Journal of Hydrology. 132(1-4):321–342.

Arusha Region Water Master Plan (AWMP). 2000. Part II of the Plan: Plans proposed for implementation; Volume 6: Water Supply Planning, Hanang District, Final Report. United Republic of Tanzania: United Nation Development Programme.

Bako MD, Owoade A. 1988. Field application of a numerical method for the derivation of baseflow recession constant. Hydrological Processes. 2(4):331–336.

Bedient PB, Huber WC, Vieux BE. 2002. Hydrology and Floodplain Analysis. New Jersey: Prentice Hall.

Beven KJ. 2006. Rainfall-Runoff Modeling: Introduction. In: Anderson M, McDonnell J, editors. Encyclopedia of Hydrological Sciences. Chichester, UK: John Wiley & Sons, Ltd.

Boussinesq J. 1904. Recherges theoretique sur l'ecoulement des nappes d'eau infiltrees dans le sol et sur le debit des sources. Journal des Mathematiques Pures et Appliquees. 10(5):5-78,363-369.

Brandes D, Hoffmann JG, Mangarillo JT. 2005. Base Flow Recession Rates, Low Flows, and Hydrologic Features of Small Watersheds in Pennsylvania, USA. Journal of the Astronomical Society of Western Australia. 41:1177–1186.

Bryan K. 1919. Classification of springs. The Journal of Geology. 27(7):522–561.

Conway D, Hanson CE, Doherty R, Persechino A. 2007. GCM simulations of the Indian Ocean dipole influence on East African rainfall: Present and future. Geophysical Research Letters. 34:L03705.

Darling WG, Gizaw B, Arusei MK. 1996. Lake-groundwater relationships and fluid-rock interaction in the East African Rift Valley: isotopic evidence. Journal of African Earth Sciences. 22(4):423–431.

Dawson JB. 2008. The Gregory Rift Valley and Neogene-Recent Volcanoes of Northern Tanzania. London: Geological Society.

Dingman SL. 2002. Physical Hydrology. 2nd ed. New Jersey: Prentice Hall.

Dupuit J. 1863. Estudes Thèoriques et Pratiques sur le mouvement des Eaux dans les canaux dècouverts et à travers les terrains permèables. 2nd ed. Paris: Dunod.

Fetter CW. 2001. Applied Hydrogeology. 3rd ed. New Jersey: Prentice Hall.

Ghiglieri G, Balia R, Oggiano G, Pittalis D. 2009. Prospecting for safe (low fluoride) groundwater in the eastern African Rift: a multidisciplinary approach in the Arumeru District (northern Tanzania). Hydrology and Earth System Sciences Discussions. 6(6):7321–7348.

Gleick PH. 1987. The development and testing of a water balance model for climate impact assessment: modeling the Sacramento basin. Water Resources Research. 23(6):1049–1061.

Greenway PJ. 1955. Ecological observations on an extinct East African volcanic mountain. The Journal of Ecology. 43(2):544–563.

Hall FR. 1968. Base-flow recessions- A review. Water Resources Research. 4(5):973–983.

Hulme M, Doherty R, Ngara T, New M, Lister D. 2001. African climate change: 1900-2100. Climate Research. 17(2):145–168.

International Atomic Energy Agency and World Meteorological Organization (IAEA/WMO) [Internet]. 2006. Vienna, Austria: International Atomic Energy Agency. Global Network of Isotopes in Precipitation: The GNIP Database; [cited 2011 March 3]. Available from: http://www-naweb.iaea.org/napc/ih/IHS_resources_gnip.html

Japan International Cooperation Agency (JICA). 2008. The study on the groundwater resources development and management in the Internal Drainage Basin in the United Republic of Tanzania. Arusha, Tanzania: JICA.

Jiang T, Chen YD, Xu C, Chen X, Singh VP. 2007. Comparison of hydrological impacts of climate change simulated by six hydrological models in the Dongjiang Basin, South China. Journal of Hydrology. 336(3-4):316–333.

Kabanda TA, Jury MR. 1999. Inter-annual variability of short rains over northern Tanzania. Climate Research. 13(3):231–241.

Kendall C, McDonnell JJ. 1998. Isotope Tracers in Catchment Hydrology. Amsterdam:

Elsevier.

Kilsby CG, Cowpertwait PS, O'Connell PE, Jones PD. 1998. Predicting rainfall statistics in England and Wales using atmospheric circulation variables. International Journal of Climatology. 18(5):523–539.

Krause P, Boyle DP, Bäse F. 2005. Comparison of different efficiency criteria for hydrological model assessment. Advances in Geosciences. 5:89–97.

Lamb R, Beven K. 1997. Using interactive recession curve analysis to specify a general catchment storage model. Hydrology and Earth System Sciences. 1(1): 101–113.

Leavesley GH. 1994. Modeling the effects of climate change on water resources- a review. Climatic Change. 28(1):159–177.

Legates DR, McCabe Jr. GJ. 1999. Evaluating the use of "goodness-of-fit" measures in hydrologic and hydroclimatic model validation. Water Resources Research. 35(1):233–241.

Manga M. 2001. Using springs to study groundwater flow and active geologic processes. Annual Review of Earth and Planetary Sciences. 29(1): 201–228.

Mckenzie JM, Mark BG, Thompson LG, Schotterer U, Lin PN. 2010. A hydrogeochemical survey of Kilimanjaro (Tanzania): implications for water sources and ages. Hydrogeology Journal. 18(4):985–995.

Mendoza GF, Steenhuis TS, Walter MT, Parlange JY. 2003. Estimating basin-wide hydraulic parameters of a semi-arid mountainous watershed by recession-flow analysis. Journal of Hydrology. 279(1-4):57–69.

Moore GK. 1992. Hydrograph analysis in a fractured rock terrane. Ground Water. 30(3):390–395.

Mul ML, Mutiibwa RK, Foppen JW, Uhlenbrook S, and Savenije HH. 2007. Identification of groundwater flow systems using geological mapping and chemical spring analysis in South Pare Mountains, Tanzania. Physics and Chemistry of the Earth, Parts A/B/C. 32(15-18):1015–1022.

Nash JE, Sutcliffe JV. 1970. River flow forecasting through conceptual models part I–A discussion of principles. Journal of Hydrology. 10(3):282–290.

Nicholson SE. 2001. Climatic and environmental change in Africa during the last two centuries. Climate Research. 17(2):123–144.

Oreste. 2010. Personal Communication. Gendabi, Tanzania.

Paeth H, Hense A. 2006. On the linear response of tropical African climate to SST changes deduced from regional climate model simulations. Theoretical and Applied Climatology. 83(1):1–19.

Parry ML. 2007. Climate Change 2007: impacts, adaptation and vulnerability: contribution of Working Group II to the fourth assessment report of the Intergovernmental Panel on Climate Change. UK: Cambridge University Press.

Ropelewski CF, Halpert MS. 1996. Quantifying southern oscillation-precipitation relationships. Journal of Climate. 9(5):1043–1059.

Schreck CJ, Semazzi FH. 2004. Variability of the recent climate of eastern Africa. International Journal of Climatology. 24(5): 681-701.

Shonsey CW. 2009. Quantifying Available Water at the Village Level: A Case Study of Horongo, Mali, West Africa. M.S. Report. Houghton, MI: Michigan Technological University.

Smakhtin VU. 2001. Low flow hydrology: a review. Journal of Hydrology. 240(3-4):147–186.

Tallaksen LM. 1995. A review of baseflow recession analysis. Journal of Hydrology. 165(1-4):349–370.

Thomas CM. 1966. Quarter degree sheet 84, "Hanang". Tanzania Geological Survey Series 1:125,000. Dodoma, Tanzania: Tanzania Geological Survey.

Thornthwaite CW. 1948. An approach toward a rational classification of climate. Geographical Review. 38(1):55–94.

Thornthwaite CW, Mather JR. 1955. The water balance. Climatology. 8: 1-104.

Ummenhofer CC, Gupta AS, England MH, Reason CJ. 2009. Contributions of Indian Ocean sea surface temperatures to enhanced East African rainfall. Journal of Climatology. 22:993–1013.

Varis O, Kajander T, Lemmelä R. 2004. Climate and water: from climate models to water resources management and vice versa. Climatic Change. 66(3):321–344.

World Health Organization (WHO). 2003. Fluoride in drinking-water. Background document for preparation of WHO Guidelines for drinking-water quality. Geneva: World Health Organization.

Williams AP, Funk C. 2011. A westward extension of the warm pool leads to a westward extension of the Walker circulation, drying eastern Africa. Climate Dynamics. 1–19.

Wittenberg H. 1999. Baseflow recession and recharge as nonlinear storage processes. Hydrological Processes. 13:715–726.

Wittenberg H, Sivapalan M. 1999. Watershed groundwater balance estimation using streamflow recession analysis and baseflow separation. Journal of Hydrology. 219(1-2):20-33.

Xu CY. 1999. Climate change and hydrologic models: A review of existing gaps and recent research developments. Water Resources Management. 13(5):369–382.

Xu CY, Singh VP. 1998. A review on monthly water balance models for water resources investigations. Water Resources Management. 12(1):20–50.

Xu CY, Singh VP. 2004. Review on regional water resources assessment models under stationary and changing climate. Water Resources Management. 18(6):591–612.

Zecharias YB, Brutsaert W. 1988. Recession characteristics of groundwater outflow and base flow from mountainous watersheds. Water Resources Research. 24(10):1651–1658.

8   APPENDICES

8.1   University of Texas Copyright Information

Located: (http://www.lib.utexas.edu/usage_statement.html)

Accessed: April 27, 2011

Library Web Material Usage Statement

Public Domain

Materials that are in the public domain (such as images from the Portrait Gallery or most of the maps in the PCL Map Collection), are not copyrighted and no permission is needed to copy them. You may download them and use them as you wish. We appreciate you giving this site credit with the phrase:

"Courtesy of the University of Texas Libraries, The University of Texas at Austin."

8.2   Tanzania Geological Survey Permission

This email dialogue establishes permission for the use of Figure 2.3 (geologic map):

Re: GEOLOGICAL MAP QDS 84 HANANG   Wednesday, April 27, 2011 8:53:55 AM

From: eluhoko@yahoo.com
  To: refish@mtu.edu

Dear Randall Fish

Thanks for your mail and being sincere with our data ,actually i remember you very well when we met here at the Geological Survey of Tanzania in 2009; Now concerning your request i talked to my Director who had no objection for your academic purpose you are allowed to use it as requested.

Thanks
Ernest
--- On **Mon, 4/25/11, Randall Fish** *<refish@mtu.edu>* wrote:

> From: Randall Fish <refish@mtu.edu>
> Subject: Re: GEOLOGICAL MAP QDS 84 HANANG
> To: "Ernest Luhoko" <eluhoko@yahoo.com>
> Date: Monday, April 25, 2011, 5:15 PM
>
> Ernest,
>
> How have you been? I'm not sure if you'll remember me, I met with you briefly in 2009 and bought a couple of geologic maps.
>
> I am finishing my Master's Research at Michigan Technological University and am requesting your permission to reproduce a section of the geologic map "QDS 84 Hanang", see attachment, in my thesis entitled "USING WATER BALANCE MODELS TO APPROXIMATE THE EFFECTS OF CLIMATE CHANGE ON SPRING CATCHMENT DISCHARGE: MT. HANANG, TANZANIA."
>
> The requested permission extends to any future revisions and editions of my dissertation, including non-exclusive world rights in all languages, and to the prospective publication of my dissertation by UMI. These rights will in no way restrict republication of the material in any other form by you or by others authorized by you. Your signing of this letter will also confirm that you own [or your company owns] the copyright to the above-described material.
>
> Thank you very much for all you assistance na Mungu akubariki sana.
>
> --
> Randall Fish
> Masters International Candidate in Geological Sciences
> Michigan Technological University

8.3 U.S. Geological Survey Copyright Information

Located: (http://www.usgs.gov/laws/info_policies.html)

Accessed: April 27, 2011

Copyrights and Credits

USGS-authored or produced data and information are considered to be in the U.S. public domain. While the content of most USGS Web pages is in the U.S. public domain, not all information, illustrations, or photographs on our site are. Some non USGS photographs, images, and/or graphics that appear on USGS Web sites are used by the USGS with permission from the copyright holder. These materials are generally marked as being copyrighted. To use these copyrighted materials, you must obtain permission from the copyright holder under the copyright law.

8.4 Isotope Data

Neither stable isotope exhibited changes in concentration far outside the margin of sampling error of $\delta^{18}O\pm0.08$ and $\delta^2H \pm0.30$. There is, though, a slight enrichment of deuterium as the dry season progresses. The isotopic abundances deviate significantly when compared to the Dar es Salaam meteoric water line (MWL) ($\delta^2H=7.05\ \delta^{18}O+7.0$) from IAEA/WMO (2006), but plot closer to the Kenya Rift MWL ($\delta^2H=5.56\ \delta^{18}O+2.04$) developed by Darling et al (1996) (see Figure 8.1). While initially this might suggest precipitation origins, local precipitation has not been sampled for isotopic abundances, so concluding which MWL the original precipitation is best represented by is impossible. Also, since Jandu catchment lies on the leeward side of Mt. Hanang, precipitation patterns and potentially isotopic concentrations are strongly impacted by orographic anomalies. The slight enrichment over time of δ^2H could suggest evaporative losses from shallow soil moisture, but Kendall and McDonnell (1998) note that enrichment could also occur before rainfall infiltrates, so conclusions from the enrichment are impractical. Hence, no real supportive evidence is derived from the data, but is presented should someone undertake future isotopic research in the region (see Table 8.1).
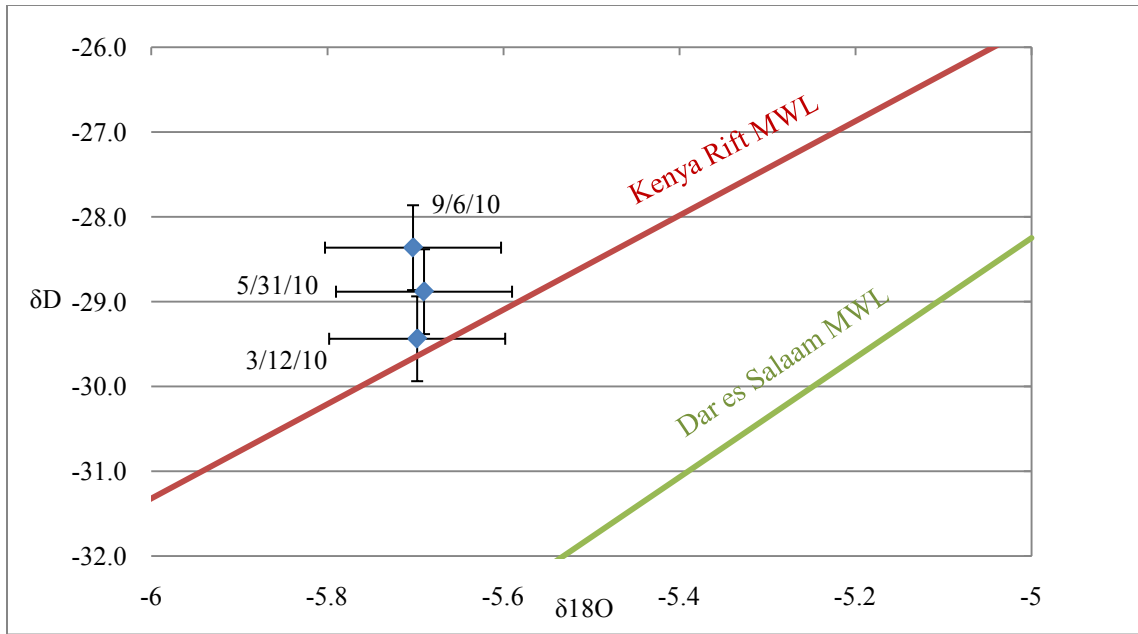
Figure 8.1 Isotopic abundances for Jandu stream

Table 8.1
Isotope data for Jandu and two other Hanang water sources

Sample ID	Sample Date	δD	StDev	δ18O	StDev
Gendabi Spring 7	3/12/2010	-28.296	0.307	-5.507	0.125
Gendabi Spring 8	6/4/2010	-27.290	0.440	-5.390	0.092
Gendabi Spring 9	9/5/2010	-27.024	0.331	-5.351	0.023
Himet Stream 5	3/15/2010	-25.694	0.465	-5.485	0.064
Himet Stream 8	6/5/2010	-26.854	0.312	-5.661	0.059
Himet Stream 10	9/7/2010	-27.134	0.288	-5.695	0.051
Jandu 4	3/12/2010	-29.438	0.353	-5.698	0.052
Jandu 5	5/31/2010	-28.883	0.252	-5.690	0.093
Jandu 7	9/6/2010	-28.364	0.282	-5.703	0.084

8.5 Thornthwaite-Mather Water Balance Equations

Governing equations are adapted from Shonsey (2009):

$$\text{If } P_m \geq PET_m \text{ then } ET_m = PET_m, \text{ but if } P_m < PET_m \text{ then } ET_m = P_m - \Delta SOIL_m$$

$$\Delta SOIL_m = SOIL_m - SOIL_{m-1}$$

$$SOIL_m = SOIL_{m-1}\left[\exp\left(-\frac{PET_m - P_m}{SOIL_{max}}\right)\right]$$

$$SOIL_{max} = \theta_{fc} Z_{fc}$$

where:

P_m = Monthly precipitation (mm)

PET_m = Monthly potential evapotranspiration (mm)

ET_m = Monthly actual evapotranspiration (mm)

$\Delta SOIL$ = Monthly change in soil moisture (mm)

$SOIL_m$ = Present month's estimated soil moisture (mm)

$SOIL_{m-1}$ = *Previous month's estimated soil moisture (mm)

$SOIL_{max}$ = Maximum achievable soil moisture (mm)

θ_{fc} = Field capacity of the soil (mm)

Z_{fc} = Vertical extent of the root zone (mm)

*To start calculations $SOIL_{m-1}$ is equal to $SOIL_{max}$

Potential evapotranspiration (*PET*) is calculated by the Hamon method:

$$PET = 924 \cdot D \cdot \frac{e_a^*(T_a)}{T_a + 273.2}$$

where:

> PET = potential evapotranspiration (mm/month)
>
> D = day length (hr)
>
> e_a^* = saturation vapor pressure at the mean daily temperature (kPa)
>
> T_a = mean daily temperature (°C)

Saturation vapor pressure is estimated as (Dingman 2002):

$$e_a^*(T_a) = 0.611\exp\left(\frac{17.3T_a}{T^a + 237.3}\right)$$

Day length is calculated with the following equation sets (Dingman 2002):

$$\Gamma = \frac{2\pi(J-1)}{365}$$

$$\delta = 0.006918 - 0.399912\cos(\Gamma) + 0.070257\sin(\Gamma) - 0.006758\cos(2\Gamma)$$
$$+ 0.000907\sin(2\Gamma) - 0.002697\cos(3\Gamma) + 0.00148\sin(3\Gamma)$$

$$D = 2\left(\frac{\cos^{-1}\left[-\tan(\delta)\tan(\Lambda)\right]}{\omega}\right)$$

where:

> Γ = day angle (radians)
>
> J = day number (Julian days)
>
> δ = sun declination (radians)
>
> Λ = latitude (radians)
>
> ω = earth's angular velocity (0.2618 radians/hr)

8.6 Katesh Precipitation Data

Ry	Sep	Oct	Nov	Dec	Jan	Feb	Mar	Apr	May	Jun	Jul	Aug	TOTAL
1985	3	14	147	84	0	90	88	82	60	0	0	0	568
1986	0	0	113	106	183	21	284	140	90	0	0	0	937
1987	0	0	35	159	228	99	75	128	98	33	0	0	855
1988	0	0	23	56	168	70	126	87	0	0	0	0	530
1989	0	0	0	87	324	151	266	151	41	0	0	0	1020
1990	0	12	63	242	35	123	97	137	3	0	0	2	714
1991	0	0	0	99	84	31	260	50	45	0	0	0	569
1992	0	3	6	183	41	189	63	129	48	0	0	0	662
1993	0	0	95	111	146	124	208	13	11	0	0	0	707
1994	0	0	0	111	102	128	62	5	47	0	0	0	455
1995	0	2	45	37	65	133	136	31	115	0	0	0	564
1996	0	0	0	55	93	348	177	252	22	0	0	0	947
1997	0	32	0	44	123	235	50	109	92	27	0	0	711
1998	0	30	260	628	364	245	122	162	51	6	0	0	1868
1999	0	0	11	1	170	40	326	139	12	6	0	0	705
2000	0	0	3	0	0	28	0	0	0	0	0	30	60
2001	0	0	1	0	168	75	167	43	0	0	18	0	471
2002	11	0	19	80	226	107	146	71	89	0	0	6	756
*2003	6	22	27	138	129	109	104	92	27	4	0	1	660
2004	3	6	61	126	154	123	50	83	3	0	0	0	609
2005	45	2	17	120	76	60	104	101	0	0	0	0	524
2006	0	10	0	8	36	139	228	51	4	0	0	2	476
2007	4	118	337	235	92	89	33	37	0	0	0	5	949
2008	0	1	9	64	235	92	84	33	35	0	0	0	552
2009	5	0	73	112	56	140	78	70	3	0	0	0	537
2010	0	0	97	220	136	108	177	50	93	0	0	0	881

Precipitation data is millimeters

Ry is rainyear (Ry 1985 is September 1984 to August 1985)

*2003 data is the mean precipitation for that month for the record.

8.7 Jandu Monthly Discharge Data

Ry	Sep	Oct	Nov	Dec	Jan	Feb	Mar	Apr	May	Jun	Jul	Aug	TOTAL
1991	nd	nd	nd	nd	nd	nd	nd	nd	38,636	29,889	28,870	26,575	123,970
1992	23,952	22,070	20,995	28,685	30,586	31,709	nd	nd	nd	nd	nd	nd	157,997
1993	nd	nd	35,338	53,309	21,773	15,293	16,848	12,960	12,960	10,368	10,714	10,714	200,275
1994	10,368	8,035	7,949	8,035	10,109	11,318	16,243	15,725	17,712	9,677	8,035	8,035	131,242
1995	6,566	5,357	6,912	24,710	21,168	23,674	44,582	25,747	26,957	18,662	13,478	13,392	231,206
1996	10,368	10,714	10,368	10,541	12,614	21,600	22,896	57,802	35,424	20,390	17,366	16,070	246,154
1997	12,960	13,133	10,541	17,021	nd	nd	nd	nd	nd	nd	nd	nd	53,654

Ry	Sep	Oct	Nov	Dec	Jan	Feb	Mar	Apr	May	Jun	Jul	Aug	TOTAL
2005	12,138	12,670	12,039	30,962	29,968	27,729	35,057	26,130	24,571	19,672	17,477	14,413	262,825
2006	11,846	9,611	10,320	9,855	15,606	16,415	29,517	44,753	56,470	18,716	14,833	12,643	250,585
2007	11,084	9,369	14,221	68,430	90,658	112,003	91,226	46,316	73,543	42,441	34,961	33,896	628,149
2008	30,664	25,628	24,267	39,006	31,307	38,215	56,400	47,693	40,211	29,520	25,628	22,522	411,061
2009	20,778	19,860	23,532	25,121	26,091	29,632	33,674	60,061	23,738	18,162	17,192	13,413	311,253
2010	10,299	9,198	19,500	45,692	54,087	25,799	55,736	44,247	37,581	25,196	20,235	17,537	365,108

Ry is rainyear, discharges are in cubic meters, and nd is no data

53

8.8 Jandu Water Geochemistry Reports

MICHIGAN DEPARTMENT OF COMMUNITY HEALTH
UPPER PENINSULA LABORATORY
USEPA Region V Drinking Water Cert. No. MI00035
P.O. Box 38
Houghton, MI 49931
TEL: (906) 487-3011
FAX: (906) 487-3682

Official Laboratory Report

Report To: JOHN GIERKE/GMES
1400 TOWNSEND DR
HOUGHTON MI 49931-1200

Sample Number: HT43021

System Name/Owner:		WSSN/Pool ID:	
Collection Address:	JANDU #8,	Source:	Other
Collected By:	FISH	Site Code:	
Township/Well#/Section:	//	Collector:	Other
County:	Unknown	Date Collected:	09/08/2010
Sample Point:		Date Received:	11/08/2010 13:55
Water System:	Other	Purpose:	Other

TESTING INFORMATION			REGULATORY INFORMATION			
Analyte Name	Result (mg/L)	Date Tested	RL (mg/L)	MCL/AL (mg/L)	Method	CAS #
Chloride	Not detected	11/09/2010	4		SM 4500-Cl E	7647-14-5
Fluoride	2.6	11/09/2010	0.1	4.0	SM 4500 FC	16984-48-8
Hardness as CaCO3	98	11/10/2010	10		SM 2340 C	HARD-00-C
Iron	Not detected	11/10/2010	0.1		SM 3500 FeB	7439-89-6
Nitrate as N	Not Detected	11/09/2010	0.4	10	SM 4500 NO3F	14797-55-8
Nitrite as N	0.06	11/09/2010	0.05	1	SM 4500 NO3F	14797-65-0
Sodium	19	11/10/2010	5		SM 3111B	7440-23-5
Sulfate	7	11/10/2010	5		SM 4500 SO4E	14808-79-8

The analyses performed by the MDCH Drinking Water Laboratory were conducted using methods approved
by the U.S. Environmental Protection Agency in accordance with the Safe Drinking Water Act, 40 CFR parts
141-143, and other regulatory agencies as appropriate.

Your local health department has detailed information about the quality of drinking water in your area. If you
have concerns about the health risks related to the test results of your sample, please contact the
Environmental Health Section through the address and telephone number listed below:

Unknown

CAS# : Chemical Abstract Service	RL : Reporting Limit	Laboratory Contacts
Registry Number	mg/L : milligrams / Liter (ppm)	Laboratory Scientist: Patricia Wheeler
MCL : Maximum Contaminant Level	ppm : parts per million	Laboratory Scientist: Roger Skufca
AL : Action Level	MPN : Most Probable Number	

By authority of PA 368 of 1978 as amended   Work Order 01100207_08   Report Created on: 11/10/2010 3:10:21PM   Page 1 of 1

MICHIGAN DEPARTMENT OF COMMUNITY HEALTH
UPPER PENINSULA LABORATORY
USEPA Region V Drinking Water Cert. No. MI00035
P.O. Box 38
Houghton, MI 49931
TEL: (906) 487-3011
FAX: (906) 487-3682

Official Laboratory Report

Report To: JOHN GIERKE/GMES
            1400 TOWNSEND DR
            HOUGHTON MI 49931-1200

Sample Number: HT43023

System Name/Owner:		WSSN/Pool ID:		
Collection Address:	JANDU #6,	Source:	Other	
Collected By:	FISH	Site Code:		
Township/Well#/Section:	//	Collector:	Other	
County:	Unknown	Date Collected:	05/31/2010	
Sample Point:		Date Received:	11/08/2010	13:56
Water System:	Other	Purpose:	Other	

TESTING INFORMATION			REGULATORY INFORMATION			
Analyte Name	Result (mg/L)	Date Tested	RL (mg/L)	MCL/AL (mg/L)	Method	CAS #
Chloride	Not detected	11/09/2010	4		SM 4500-Cl E	7647-14-5
Fluoride	2.6	11/09/2010	0.1	4.0	SM 4500 FC	16984-48-8
Hardness as CaCO3	95	11/10/2010	10		SM 2340 C	HARD-00-C
Iron	Not detected	11/10/2010	0.1		SM 3500 FeB	7439-89-6
Nitrate as N	Not Detected	11/09/2010	0.4	10	SM 4500 NO3F	14797-55-8
Nitrite as N	Not detected	11/09/2010	0.05	1	SM 4500 NO3F	14797-65-0
Sodium	17	11/10/2010	5		SM 3111B	7440-23-5
Sulfate	7	11/10/2010	5		SM 4500 SO4E	14808-79-8

The analyses performed by the MDCH Drinking Water Laboratory were conducted using methods approved by the U.S. Environmental Protection Agency in accordance with the Safe Drinking Water Act, 40 CFR parts 141-143, and other regulatory agencies as appropriate.

Your local health department has detailed information about the quality of drinking water in your area. If you have concerns about the health risks related to the test results of your sample, please contact the Environmental Health Section through the address and telephone number listed below:

Unknown

CAS# : Chemical Abstract Service Registry Number	RL : Reporting Limit	Laboratory Contacts
MCL : Maximum Contaminant Level	mg/L : milligrams / Liter (ppm)	Laboratory Scientist: Patricia Wheeler
AL : Action Level	ppm : parts per million	Laboratory Scientist: Roger Skufca
	MPN : Most Probable Number	

8.9 CD Contents

- Thornthwaite-Mather Water Balance Model spreadsheet
- Model 1 spreadsheet
- Model 2 spreadsheet
- Jandu discharge data (2004-2010)
- Katesh precipitation data (1985-2010)